



UvA-DARE (Digital Academic Repository)

Search for new phenomena in the dijet mass distribution using pp collision data at $\sqrt{s} = 8$ TeV with the ATLAS detector

Aad, G.; et al., [Unknown]; Aben, R.; Angelozzi, I.; Beemster, L.J.; Bentvelsen, S.; Berge, D.; Bobbink, G.J.; Bos, K.; Boterenbrood, H.; Butti, P.; Castelli, A.; Colijn, A.P.; de Jong, P.; de Nooij, L.; Deigaard, I.; Deluca, C.; Deviveiros, P.O.; Dhaliwal, S.; Ferrari, P.; Gadatsch, S.; Geerts, D.A.A.; Hartjes, F.; Hessey, N.P.; Hod, N.; Igonkina, O.; Kluit, P.; Koffeman, E.; Lee, H.; Linde, F.; Mahlstedt, J.; Mechnich, J.; Oussoren, K.P.; Pani, P.; Salek, D.; Valencic, N.; van den Wollenberg, W.; van der Deijl, P.C.; van der Geer, R.; van der Graaf, H.; van der Leeuw, R.; van Vulpen, I.; Verkerke, W.; Vermeulen, J.C.; Vreeswijk, M.; Weits, H.

DOI

[10.1103/PhysRevD.91.052007](https://doi.org/10.1103/PhysRevD.91.052007)

Publication date

2015

Document Version

Final published version

Published in

Physical Review D. Particles and Fields

[Link to publication](#)

Citation for published version (APA):

Aad, G., et al., U., Aben, R., Angelozzi, I., Beemster, L. J., Bentvelsen, S., Berge, D., Bobbink, G. J., Bos, K., Boterenbrood, H., Butti, P., Castelli, A., Colijn, A. P., de Jong, P., de Nooij, L., Deigaard, I., Deluca, C., Deviveiros, P. O., Dhaliwal, S., ... Weits, H. (2015). Search for new phenomena in the dijet mass distribution using pp collision data at $\sqrt{s} = 8$ TeV with the ATLAS detector. *Physical Review D. Particles and Fields*, 91(5), [052007]. <https://doi.org/10.1103/PhysRevD.91.052007>

General rights

It is not permitted to download or to forward/distribute the text or part of it without the consent of the author(s) and/or copyright holder(s), other than for strictly personal, individual use, unless the work is under an open content license (like Creative Commons).

Search for new phenomena in the dijet mass distribution using pp collision data at $\sqrt{s} = 8$ TeV with the ATLAS detector

G. Aad *et al.**

(ATLAS Collaboration)

(Received 8 July 2014; published 9 March 2015)

Dijet events produced in LHC proton-proton collisions at a center-of-mass energy $\sqrt{s} = 8$ TeV are studied with the ATLAS detector using the full 2012 data set, with an integrated luminosity of 20.3 fb^{-1} . Dijet masses up to about 4.5 TeV are probed. No resonancelike features are observed in the dijet mass spectrum. Limits on the cross section times acceptance are set at the 95% credibility level for various hypotheses of new phenomena in terms of mass or energy scale, as appropriate. This analysis excludes excited quarks with a mass below 4.06 TeV, color-octet scalars with a mass below 2.70 TeV, heavy W' bosons with a mass below 2.45 TeV, chiral W^* bosons with a mass below 1.75 TeV, and quantum black holes with six extra space-time dimensions with threshold mass below 5.66 TeV.

DOI: [10.1103/PhysRevD.91.052007](https://doi.org/10.1103/PhysRevD.91.052007)

PACS numbers: 13.85.Rm, 12.60.Rc, 13.87.Ce, 14.80.-j

I. INTRODUCTION

This paper describes the search for new phenomena (NP) in the two-jet (dijet) invariant mass spectrum in the full 2012 data set delivered by the Large Hadron Collider (LHC) at CERN, and collected with the ATLAS detector. The studies reported here select events containing two or more jets. The two highest- p_T (“leading” and “subleading”) jets are combined to determine the dijet invariant mass, m_{jj} . High-transverse-momentum (high- p_T) dijet events are produced copiously by QCD processes, and can reach the highest mass scales accessible in LHC pp collisions. The QCD processes, along with a subpercent admixture of additional Standard Model (SM) processes, create a smooth rapidly falling spectrum in m_{jj} . Many NP models describe new particles or excitations created as s -channel resonances with appreciable branching ratios to final states involving quarks and gluons (q and g), and can produce dijet final states. If the resonance width is sufficiently narrow, these NP signals would appear as local excesses (bumps) in the dijet mass spectrum over the smooth SM background.

Studies searching for excesses in dijet mass spectra have been performed in all previous collider experiments, including CDF and D0 at the Tevatron [1–4]. At the LHC, the CMS and ATLAS experiments have continued this program, starting from the first 2010 data [5–14]. The most recent published ATLAS results used the 2011 data set of 4.8 fb^{-1} at a center-of-mass energy of $\sqrt{s} = 7$ TeV [13]. In 2012, the LHC delivered an integrated luminosity

of 20.3 fb^{-1} [15] in proton-proton (pp) collisions, roughly a factor of 4 more than used for previous dijet studies. In addition, the increase in center-of-mass energy to $\sqrt{s} = 8$ TeV in 2012 increased the sensitivity in searches for new phenomena, and pushed exclusion limits to higher masses and energy scales. This increased kinematic reach, combined with a new online event selection strategy employed in the present analysis, provides the largest dijet invariant mass range coverage to date, from 250 GeV to 4.5 TeV.

No significant excess is observed above the background. A number of NP models are compared to data to derive limits. The models chosen span a range of characteristic masses (or energy scales) and cross sections, and are complementary in terms of the flavor of their final-state partons. The benchmark models under consideration include excited quarks (q^*) decaying to qg [16,17], color-octet scalars (s_8) decaying to gg [18–21], heavy W' gauge bosons decaying to $q\bar{q}'$ [22–29], two forms of chiral W^* gauge bosons [30–33] and quantum black holes [34–37] decaying to a mixture of quarks and gluons. The current dijet search also sets limits on new generic resonances whose intrinsic width is convolved with effects due to parton distribution functions (PDFs), parton shower, nonperturbative effects and detector resolution.

II. THE ATLAS DETECTOR

A detailed description of the ATLAS detector has been published elsewhere [38]. The detector is instrumented over almost the entire solid angle around the pp collision point with layers of tracking detectors, calorimeters, and muon chambers.

In ATLAS, high- p_T hadronic jets are measured using a finely segmented calorimeter system, designed to achieve high reconstruction efficiency and excellent energy resolution. Electromagnetic calorimetry is provided by high-granularity liquid-argon (LAr) sampling calorimeters,

* Full author list given at the end of the article.

Published by the American Physical Society under the terms of the *Creative Commons Attribution 3.0 License*. Further distribution of this work must maintain attribution to the author(s) and the published articles title, journal citation, and DOI.

using lead as an absorber. The calorimeters are split into a barrel region ($|\eta| < 1.475$) and two end-cap ($1.375 < |\eta| < 3.2$) regions.¹ The hadronic calorimeter is divided into barrel, extended barrel ($|\eta| < 1.7$) and end-cap ($1.5 < |\eta| < 3.2$) regions. The barrel and extended barrel are instrumented with scintillator tiles and steel absorbers, while the end-caps use copper with LAr modules. The forward calorimeter ($3.1 < |\eta| < 4.9$) is instrumented with modules using LAr as the active medium and copper or tungsten as absorbers to provide electromagnetic and hadronic energy measurements, respectively.

III. JET AND EVENT SELECTION

Jets are reconstructed from contiguous groups of calorimeter cells that contain significant energy above noise (topological clusters) [39]. The anti- k_r jet algorithm [40,41] is applied to these clusters using a distance parameter of $R = 0.6$. Effects from additional pp interactions in the same and neighboring bunch crossings are corrected for using the calibration procedure described in Ref. [42]. Simulated QCD multijet events are used for the derivation of the jet calibration to the hadronic scale. They are produced with the event generator PYTHIA [43] 8.160, using the CT10 PDF [44] and the AU2 set of parameters to describe the nonperturbative effects tuned to ATLAS data (the AU2 tune) [45]. Detector effects are simulated using GEANT4 within the ATLAS software infrastructure [46,47]. Additional simulated minimum-bias events are overlaid onto the hard scattering, both within the same bunch crossings and within trains of consecutive bunches. The same software used to reconstruct data is used for the Monte Carlo (MC) samples. The level of agreement between data and MC simulation is further improved by the application of calibration constants obtained with *in situ* techniques based on momentum balancing between central and forward jets, between photons or Z bosons and jets, and between high-momentum jets and a recoil system of low-momentum jets [48].

The energy scale of central jets relevant to this search is known to within 4% [48]. The jet energy resolution is estimated both in data and in simulation using transverse momentum balance studies in dijet events [49], and are found to be in agreement within uncertainties. The dijet mass resolution is approximately 8% at 200 GeV, and improves to less than 4% above 2 TeV. The measured dijet mass distribution is not corrected for detector resolution effects.

¹ATLAS uses a right-handed coordinate system with its origin at the nominal interaction point (IP) in the center of the detector and the z axis along the beam pipe. The x axis points from the IP to the center of the LHC ring, and the y axis points upward. Cylindrical coordinates (r, ϕ) are used in the transverse plane, ϕ being the azimuthal angle around the beam pipe. The pseudorapidity is defined in terms of the polar angle θ as $\eta = -\ln \tan(\theta/2)$.

The data were collected using single-jet triggers [50]. These triggers are designed to select events that have at least one large transverse energy deposition in the calorimeter. To match the data rate to the processing and storage capacity available to ATLAS, the triggers with low- p_T thresholds are prescaled; only a preselected fraction of all events passing the threshold is recorded. Combinations of prescaled single-jet triggers are used to reach lower dijet invariant masses. The highest prescale for the trigger combinations used in this analysis is 1/460000. This trigger combination is used for jets with p_T between 59 and 99 GeV.

For a given leading-jet p_T , a predetermined combination of triggers with efficiencies exceeding 99.5% is used to select the event. Each event is weighted according to the average effective integrated luminosity recorded by the given trigger combination [51].

During the 2012 data taking, ATLAS recorded data at a rate that was higher than the rate of the offline reconstruction: 400 Hz of recorded data were promptly reconstructed, while 100 Hz of data from hadronic triggers were recorded and reconstructed later (the “delayed stream”). Dijet events from the delayed data stream fall primarily into the region between 750 GeV and 1 TeV. They are used to further increase the size of the analysis data set as follows. First, two independent data sets are built from the delayed and normal trigger streams. The m_{jj} distributions from the two data sets have been checked to be in agreement with a shape-only Kolmogorov-Smirnov test, leading to a probability of 86% for their compatibility. The two dijet mass distributions measured from these data sets are then averaged, using the effective integrated luminosity as a weight. The delayed stream increases the luminosity recorded in this region of phase space by up to an order of magnitude. The effective integrated luminosity attained in this analysis (using the 2012 normal stream with the added delayed stream) is compared to previous ATLAS analyses in Fig. 1.

Events used for the search are required to have at least one collision vertex defined by two or more charged-particle tracks. In the presence of multiple pp interactions, the collision vertex with the largest scalar sum of p_T^2 of its associated tracks is chosen as the primary vertex.

Events are rejected if either the leading jets, or any of the other jets with p_T greater than 30% of the p_T of the subleading jet, are poorly measured or have a topology characteristic of noncollision background or calorimeter noise [52]. Poorly measured jets correspond to energy depositions in regions where the energy measurement is known to be inaccurate. Events are also rejected if one of the jets relevant to this analysis falls into regions of the calorimeter that were nonoperational during data taking. An inefficiency of roughly 10% due to this veto is emulated in MC signal samples following the same conditions as data. Central values and statistical errors of the dijet mass

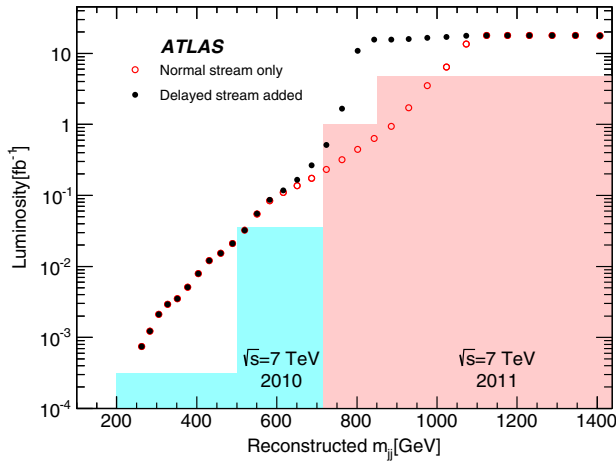


FIG. 1 (color online). Recorded effective integrated luminosity as a function of dijet mass for all former ATLAS dijet searches (shaded boxes). The integrated luminosity per dijet mass bin from the 2012 data used in the current analysis is shown without (open circles) and with (filled circles) the added delayed data stream.

spectra of both the data and MC signal samples are scaled, in order to correct for this inefficiency.

Additional kinematic selection criteria are used to enrich the dijet sample with events in the hard-scatter region of phase space. The rapidity y of the two leading jets must be within $|y| < 2.8$. The leading and subleading jets are required to have a $p_T > 50$ GeV, ensuring a jet reconstruction efficiency of 100% [53] both for QCD background and for all benchmark models under consideration. Events must satisfy $|y^*| = \frac{1}{2}|y_{\text{lead}} - y_{\text{sublead}}| < 0.6$ and $m_{jj} > 250$ GeV. The invariant mass cut of $m_{jj} > 250$ GeV is chosen such that the dijet mass spectrum is unbiased by the kinematic selection on p_T .

IV. COMPARISON OF THE DIJET MASS SPECTRUM TO A SMOOTH BACKGROUND

The observed dijet mass distribution in data, after all selection requirements, is shown in Fig. 2. The bin width varies with mass and is chosen to approximately equal the dijet mass resolution derived from simulation of QCD processes. The predictions for an excited quark q^* with three different mass hypotheses are also shown.

The search for resonances in m_{jj} uses a data-driven background estimate derived by fitting a smooth functional form to the spectrum. An important feature of this functional form is that it allows for smooth background variations, but does not accommodate localized excesses that could indicate the presence of NP signals. In previous studies, ATLAS and other experiments [54] have found that the following function provides a satisfactory fit to the QCD prediction of dijet production:

$$f(x) = p_1(1-x)^{p_2}x^{p_3+p_4 \ln x}, \quad (1)$$

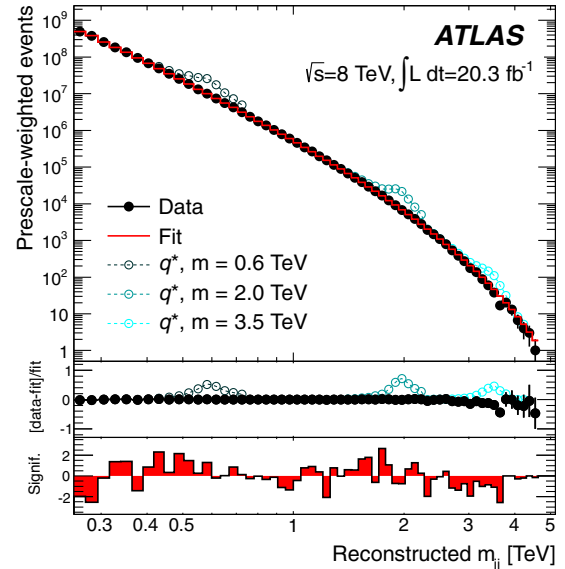


FIG. 2 (color online). The reconstructed dijet mass distribution (filled points) fitted with a smooth functional form (solid line). Predictions for three q^* masses are shown above the background. The central panel shows the relative difference between the data and the background fit with overlaid predictions for the same q^* masses. The bin-by-bin significance of the data-background difference considering statistical uncertainties only is shown in the bottom panel.

where the p_i are fit parameters, and $x \equiv m_{jj}/\sqrt{s}$. The uncertainty associated with the stability of the fit is carried forward as a nuisance parameter in the statistical analysis.

The functional form was selected using a data set consisting of a quarter of the full data, a quantity known to be insensitive to resonant new physics at dijet masses above 1.5 TeV after the previous public result on 13 fb^{-1} of data [55]. A range of parametrizations were tested on the blinded data set using a k -fold cross-validation and there was found to be no substantial difference between the standard function of Eq. (1) and higher-order parametrizations, so the function with a simpler form and a published precedent was selected. The χ^2 value of the fit to the blinded data set was 37 for 56 degrees of freedom using the parametrization of Eq. (1). The fit function showed good agreement to both the fully simulated dijet mass spectrum obtained from the simulated PYTHIA 8.160 QCD multijet events mentioned in Sec. III, corrected for next-to-leading-order effects using the NLOJET ++v4.1.3 program [56,57] as described in Ref. [11], and from a large-statistics sample of generator-level events, for which the χ^2 of the fit was 58 for 55 degrees of freedom. While the number of data events is matched or surpassed by the number of fully simulated events starting from dijet masses of roughly 2 TeV, the generator-level statistics is sufficient to reproduce that of data. The χ^2 value of the fit to data shown in Fig. 2 is 79 for 56 degrees of freedom.

The center panel of Fig. 2 shows the relative difference between the data and the background fit, and overlays the shapes that would be expected in the presence of three sample q^* signals. The bottom panel of Fig. 2 shows the significance of the difference between the data and the fit in each bin. The significance is calculated taking only statistical uncertainties into account, and assuming that the data follow a Poisson distribution with the expected value given by the fit function.

For each bin a p -value is determined by assessing the probability of a background fluctuation leading to a number of events higher than or equal to the observed excess, or lower than or equal to the observed deficit. This p -value is converted to a significance in terms of an equivalent number of standard deviations (the z -value) [58]. Where there is an excess (deficit) in data in a given bin, the significance is plotted as positive (negative).² To test the degree of consistency between the data and the fitted background, the p -value of the fit is determined by calculating the χ^2 -value from the data and comparing this result to the χ^2 distribution obtained from pseudoexperiments drawn from the background fit, as described in a previous publication [11]. The resulting p -value is 0.027.

The BUMPHUNTER algorithm [59,60] is used to establish the presence or absence of a narrow resonance in the dijet mass spectrum, as described in greater detail in previous publications [11,12]. Starting with a two-bin window, the algorithm increases the signal window and shifts its location until all possible bin ranges, up to the widest window corresponding to half the mass range spanned by the data, are tested. The most significant excess of data above the smooth spectrum (“bump”) is defined by the set of bins over which the integrated excess of data over the fit prediction has the smallest probability of arising from a background fluctuation, assuming Poisson statistics.

The BUMPHUNTER algorithm accounts for the so-called “look-elsewhere effect” [61], by performing a series of pseudoexperiments drawn from the background estimate to determine the probability that random fluctuations in the background-only hypothesis would create an excess anywhere in the spectrum at least as significant as the one observed. Furthermore, to prevent any NP signal from biasing the background estimate, if the most significant local excess from the background fit has a p -value smaller than 0.01, the corresponding region is excluded and a new background fit is performed. The exclusion is then progressively widened bin by bin until the p -value of the

remaining fitted region is acceptable. No such exclusion is needed for the current data set.

The most significant discrepancy identified by the BUMPHUNTER algorithm in the observed dijet mass distribution in Fig. 2 is a seven-bin excess in the interval 390–599 GeV. The probability of observing an excess at least as large somewhere in the mass spectrum for a background-only hypothesis is 0.075, corresponding to a z -value of 1.44σ . To conclude, this test shows no evidence for a resonant signal in the observed m_{jj} spectrum.

V. SIMULATION OF HYPOTHETICAL NEW PHENOMENA

In the absence of any significant signals indicating the presence of phenomena beyond the SM, Bayesian 95% credibility level (C.L.) limits are determined for a number of NP hypotheses that would produce localized excesses.

Samples for NP models are produced by a variety of event generators. The partons originating from the initial $2 \rightarrow 2$ matrix elements are passed to PYTHIA 8.160 with the AU2 tune [45]. PYTHIA uses p_T -ordered parton showers to model additional radiation in the leading-logarithm approximation [62]. Multiple parton interactions [63], as well as fragmentation and hadronization based on the Lund string model [64], are also simulated. Renormalization and factorization scales for the NP models are set to the mean p_T of the two leading jets.

Excited u and d quarks (q^*), one possible manifestation of quark compositeness, are simulated in all decay modes using the PYTHIA 8.162 generator, using the CT10 PDF. Excited quarks are assumed to decay to quarks via gauge couplings set to unity, leading to a $q\bar{q}$ final state approximately 83% of the time (the remaining generated decays involve W/Z or γ emission). The acceptance, defined as the fraction of generated events passing all reconstruction steps and the analysis selection described in Sec. III using jets reconstructed from stable particles³ excluding muons and neutrinos, is approximately 58%. The largest reduction in acceptance arises from the rapidity selection criteria.

The color-octet scalar model describes the production of exotic colored resonances (s_8). MADGRAPH 5 (v1.5.5) [65] with the MSTW2008LO PDF [66] is employed to generate parton-level events at leading-order approximation. Parton showering and nonperturbative effects are simulated with PYTHIA 8.170. Color-octet scalars can decay into two gluons and can then have a broader mass distribution and larger tails than resonances decaying to quarks. For resonances produced by this model, the acceptance ranges from 61% to 63%.

The production of heavy charged gauge bosons, W' , has been sought through decays to $q\bar{q}'$. The specific model

²In mass bins with small expected number of events, where the observed number of events is similar to the expectation, the Poisson probability of a fluctuation at least as high (low) as the observed excess (deficit) can be greater than 50%, as a result of the asymmetry of the Poisson distribution. Since these bins have too few events for the significance to be meaningful, these bins are drawn with zero content.

³A stable particle is defined as one that has a lifetime longer than 10 ps.

(sequential Standard Model, or SSM [26,27]) used in this study assumes that the W' has $V - A$ SM couplings but does not include interference between the W' and the W , leading to a branching ratio to dijets of 75%. The W' signal sample is simulated with the PYTHIA 8.165 event generator using the MSTW2008LO PDF. Instead of the LO cross section values, the next-to-next-to-leading-order cross section values calculated with the MSTW2008NNLO PDF are used in this analysis, as detailed in [67] and references therein. The acceptance for W' bosons decaying to quarks ranges from 48% at masses below 1200 GeV to 40% at 3200 GeV, driven by the rapidity selection criteria. At high W' masses, the acceptance decreases due to PDF suppression effects causing the reconstructed dijet invariant mass to fall below the 250 GeV cut.

A new excited W^* boson [31,32] is generated through a simplified model [30] in the CalcHEP 3.4.2 generator, in combination with the MSTW2008LO PDF and PYTHIA 8.165 for the simulation of nonperturbative effects. The sine of the mixing angle in this model ($\sin \phi_X$) is set to zero, producing leptophobic decays of the W^* that are limited to quarks. With $\sin \phi_X = 1$, a leptophilic W^* would instead be produced with branching ratios divided equally between quarks (3 families \times 3 flavors \times 8.3%BR = 75%) and leptons (3 families \times 8.3%BR = 25%). The angular distribution of the W^* differs from that of the other signals under study, preferring decays with a wider separation in y . The acceptance for both leptophobic and leptophilic W^* spans 25% to 27%.

A model for quantum black holes (QBH) that decay to two jets is simulated using both the BLACKMAX [68] and the QBH [69] generators, to produce a simple two-body final-state scenario of quantum gravitational effects at the fundamental Planck scale M_D , with $n = 6$ extra spatial dimensions in the context of the ADD model [70]. In this model, the Planck scale is set equal to the threshold mass for the quantum black hole production m_{th} . These QBH models are used as benchmarks to represent any quantum gravitational effect that produces events containing dijets. The PDF used for the generation and parton shower of BLACKMAX is CT10, while the QBH samples employ the MSTW2008LO PDF. In the mass range considered, the branching ratio of QBH to dijets is above 85% and the acceptance is between 52% and 55% for BLACKMAX and 54%–56% for QBH. Nonperturbative effects for events coming from both event generators are simulated with PYTHIA 8.170.

Further information on cross sections, branching ratio to dijets and acceptances for the benchmark models under consideration can be found in HepData [71].

All MC signal samples except for the excited quark signals are passed through a fast detector simulation [72] with the jet calibration appropriately corrected to full simulation. The excited quark signals are simulated using GEANT4 within the ATLAS simulation infrastructure [47].

VI. LIMITS ON NEW RESONANT PHENOMENA FROM THE m_{jj} DISTRIBUTION

The Bayesian method used for the limit setting is documented in Ref. [11] and implemented using the Bayesian Analysis Toolkit [73]. Limits on the cross section times acceptance, $\sigma \times \mathcal{A}$, are set at the 95% C.L. for the NP signal as a function of m_{NP} , using a prior constant in signal strength and Gaussian priors for the nuisance parameters due to the systematic uncertainties under consideration. The full template shape is considered in the limit-setting procedure, both in the fits to the data performed during the marginalization procedure⁴ and in the likelihood for the determination of the 95% C.L. limit. The limit on $\sigma \times \mathcal{A}$ from data is interpolated linearly on the x axis and logarithmically on the y axis between the mass points to create a continuous curve in signal mass. The exclusion limit on the mass (or energy scale) of the given NP signal occurs at the value of the signal mass where the limit on $\sigma \times \mathcal{A}$ from data is the same as the theoretical value, which is derived by interpolation between the generated mass values. This form of analysis is applicable to all resonant phenomena where the NP couplings are strong compared to the scale of perturbative QCD at the signal mass, so that interference between these terms can be neglected.

As in previous dijet resonance analyses, limits on dijet resonance production are also determined using a collection of hypothetical signal shapes that are assumed to be Gaussian-distributed in m_{jj} . Signal shape templates are generated with means (m_G) ranging from 200 GeV to 4.0 TeV and with standard deviations (σ_G) corresponding to the dijet mass resolution estimated from MC simulation and ranging from 7% to 15% of the mean.⁵ For further information on the mass resolution, see Appendix B.

An additional set of limits with minimal model assumptions is added to this publication. For particles with a nonzero natural width generated at masses close to the collision energy, the parton luminosity favors lower-mass collisions. This creates an asymmetric resonance not well represented by a Gaussian distribution. To handle this scenario, Breit-Wigner signals of fixed intrinsic widths (0.5% to 5% of the resonance mass) are generated and multiplied by the parton luminosities for different initial states (qq , qg , gg and $q\bar{q}$) according to the CT10 PDF. Effects of parton shower and nonperturbative effects are

⁴The NP signal distribution is added to the binned data spectrum, and the parameters of the background function are extracted by fitting the combined distribution to a five-parameter function, where the fifth parameter is proportional to the signal strength.

⁵Limits are determined only for those Gaussian resonances whose means fall more than 2σ from either edge of the data to preserve the stability of the background estimation, so the limits from wider signals include fewer mass points near the ends of the range.

estimated using HERWIG ++ 2.6.3 [74,75] and convoluted with the signal shape.

The detector resolution is accounted for by convolving the signal shape with a Gaussian function of width equal to the detector resolution at each signal mass. The result is then truncated below 250 GeV due to the dijet mass cut. This produces a signal template shape that is still generic but more likely to match the forms visible in actual physical processes. The effect on the shape of the signal template originating from the y^* cut is not simulated in the signal templates used for these limits, due to the possible model dependence of the angular distribution of the considered NP process.⁶ Tests of the benchmark model-specific templates indicate that the combined effect of the y and y^* acceptance requirement is constant within 20% as a function of the dijet mass, with the largest discrepancies outside the mass peak.

A. Systematic uncertainties in limit setting

The effects of several systematic uncertainties are considered when setting limits on new phenomena. These are incorporated into the Bayesian marginalization limit setting procedure using Gaussian priors, with one nuisance parameter for each uncertainty. They are listed below.

- (i) Choice of fitting function: a tenfold cross validation [76] using the full data set shows that the background is also well described when introducing an additional degree of freedom to Eq. (1),

$$f(x) = p_1(1-x)^{p_2}x^{p_3+p_4 \ln x+p_5(\ln x)^2}. \quad (2)$$

The χ^2 -value of this five-parameter function fit to data is 45 for 57 degrees of freedom. Since the two fit functions provide background estimates that differ beyond statistical uncertainties, an additional uncertainty is introduced due to the choice of fitting function. The difference between the two background estimates is treated as a one-sided nuisance parameter, with a Gaussian prior centered at zero corresponding to the background estimate from Eq. (1) and truncated to one- σ corresponding to the background estimate from Eq. (2). The marginalized posterior indicates a preference for the alternative function.

- (2) Background fit quality: the uncertainty on the background parametrization from the fit is estimated by refitting bin-by-bin Poisson fluctuations of the data, as described in Ref. [77]. The resulting uncertainty is calculated by refitting a large number

⁶If a flat distribution in the jet polar angle in the center-of-mass rest frame for the new particle is assumed for the NP model, the acceptance can be calculated analytically and it amounts to roughly 56% for all considered dijet masses.

of pseudoexperiments drawn from the data, and defining the fit error from the variation in fit results in each bin: $\pm 1\sigma$ in the uncertainty corresponds to the central 68% of pseudoexperiment fit values in the bin.

- (3) Jet energy scale: shifts to the jet energy due to the various jet energy scale (JES) uncertainty components are propagated separately through the analysis of the signal templates. Changes in both shape and acceptance due to the JES uncertainty in the simulated signal templates are considered in the limit setting. Combined, the JES uncertainty shifts the resonance mass peaks by less than 3%: this is the JES shift used for Gaussian and Breit-Wigner limits.
- (4) Luminosity: a 2.8% uncertainty [15] is applied to the overall normalization of the signal templates.
- (5) Theoretical uncertainties: the uncertainty on the signal acceptance for the model-dependent limits due to the choice of PDF is derived employing the PDF4LHC recommendation [78] using the envelope of the error sets of the NNPDF 2.1 [79] and MSTW2008LO. Renormalization and factorization scale uncertainties on the signal acceptance are considered for the W' and s_8 signals but found negligible. Since the W' cross section estimation used in this analysis includes NNLO corrections, the uncertainties on cross section due to variations of the renormalization and factorization scales, the choice of PDF, and PDF + α_s variations on the theoretical cross section are considered as well.

The effect of the jet energy resolution uncertainty is found to be negligible. Similarly, effects due to jet reconstruction efficiency and jet angular resolution lead to negligible uncertainties.

B. Constraints on NP benchmark models

The resulting limits for excited quarks are shown in Fig. 3. The expected lower mass limit at 95% C.L. for q^* is 3.98 TeV, and the observed limit is 4.06 TeV. The limits for color-octet scalars are shown in Fig. 4. The expected mass limit at 95% C.L. is 2.808 TeV, and the observed limit is 2.708 TeV.

The limits for heavy charged gauge bosons, W' , are shown in Fig. 5. The expected mass limit at 95% C.L. is 2.51 TeV, and the observed limit is 2.45 TeV.

The limits for the excited W^* boson are shown in Fig. 6. The plot shows the observed and expected limits calculated for a leptophobic W^* but includes theory curves for both leptophobic and nonleptophobic W^* given that the acceptances for the two samples are the same to within 1%. The expected mass limit for the leptophobic model at 95% C.L. is 1.95 TeV and the observed limit is 1.75 TeV. The expected mass limit for the nonleptophobic model at 95% C.L. is 1.66 TeV and the observed limit is 1.65 TeV.

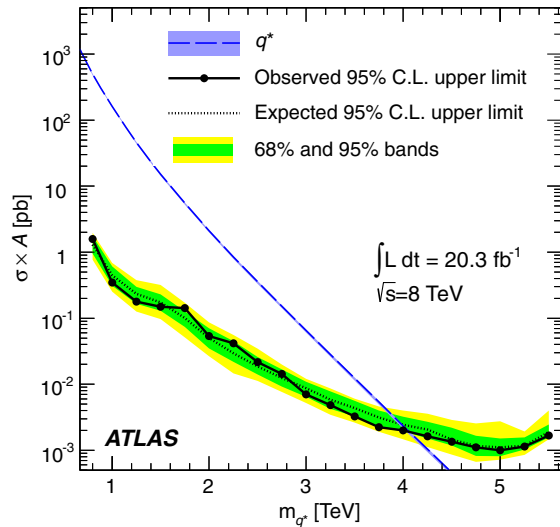


FIG. 3 (color online). Observed (filled circles) and expected 95% C.L. upper limits (dotted line) on $\sigma \times \mathcal{A}$ for excited quarks as a function of particle mass. The green and yellow bands represent the 68% and 95% contours of the expected limit. The dashed curve is the theoretical prediction of $\sigma \times \mathcal{A}$. The uncertainty on the nominal signal cross section due to the beam energy uncertainty is also displayed as a band around the theory prediction. The observed (expected) mass limit occurs at the crossing of the dashed $\sigma \times \mathcal{A}$ curve with the observed (expected) 95% C.L. upper limit curve.

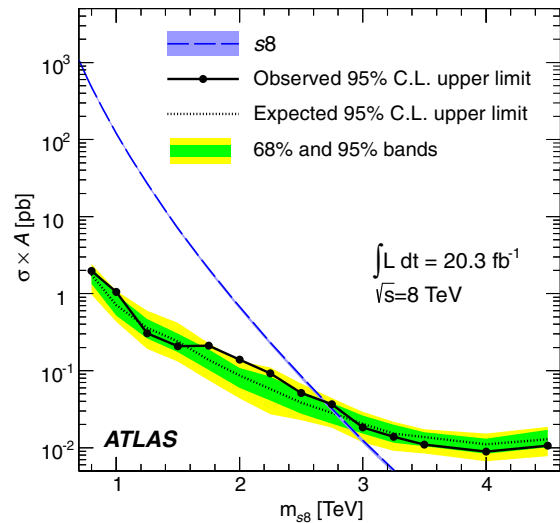


FIG. 4 (color online). Observed (filled circles) and expected 95% C.L. upper limits (dotted line) on $\sigma \times \mathcal{A}$ for color-octet scalars as a function of particle mass. The green and yellow bands represent the 68% and 95% contours of the expected limit. The dashed curve is the theoretical prediction of $\sigma \times \mathcal{A}$. The uncertainty on the nominal signal cross section due to the beam energy uncertainty is also displayed as a band around the theory prediction. The observed (expected) mass limit occurs at the crossing of the dashed $\sigma \times \mathcal{A}$ curve with the observed (expected) 95% C.L. upper limit curve.

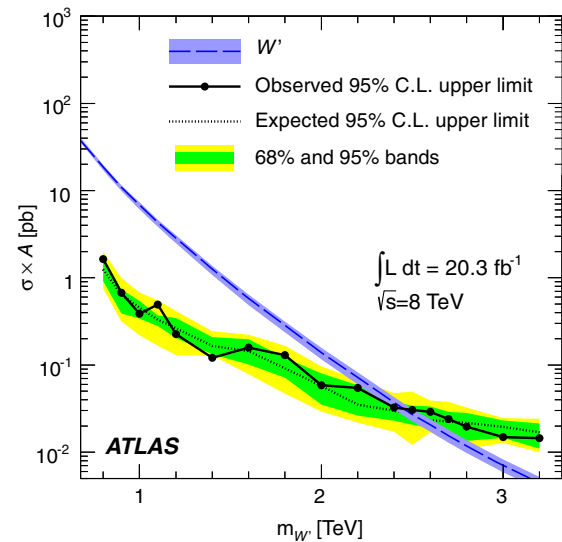


FIG. 5 (color online). Observed (filled circles) and expected 95% C.L. upper limits (dotted line) on $\sigma \times \mathcal{A}$ for heavy vector bosons as a function of particle mass. The green and yellow bands represent the 68% and 95% contours of the expected limit. The dashed curve is the theoretical prediction of $\sigma \times \mathcal{A}$. The uncertainty on the nominal signal cross section due to the beam energy uncertainty is also displayed as a band around the theory prediction. Additionally the uncertainty on the calculation of the next-to-next-to-leading order cross section is shown around the theory line. The observed (expected) mass limit occurs at the crossing of the dashed $\sigma \times \mathcal{A}$ curve with the observed (expected) 95% C.L. upper limit curve.

The limits for black holes generated using QBH and BLACKMAX are shown in Fig. 7. The observed limit is consistent between the two generators, but the cross sections differ, hence the difference in the mass limit. The observed limits for the two models have visually matching shapes and normalizations, so only one (BLACKMAX) is selected for display. The limits for both models are, however, computed separately and recorded. The expected mass limit for QBH black holes at 95% C.L. is 5.66 TeV, and the observed limit is 5.66 TeV. For BLACKMAX black holes, the expected limit at 95% C.L. is 5.62 TeV and the observed limit is 5.62 TeV. Above ~ 4.5 TeV the observed and expected limits are driven by the absence of any observed data events, leading to identical observed and expected mass limits.

Although the search phase of the analysis starts at 250 GeV, $\sigma \times \mathcal{A}$ exclusion limits on benchmark NP models are set starting at 800 GeV for the q^* , s_8 , and W' models, and at 1500 GeV for the W^* model. In the first three cases, this ensures that the rapid increase in the delayed stream statistics from 800 GeV onwards does not shift the search to be more sensitive to the tails of the model, rather than to its peak. In the W^* model, the limited acceptance distorts the peak shape below 1500 GeV so that it cannot be adequately treated as a resonance.

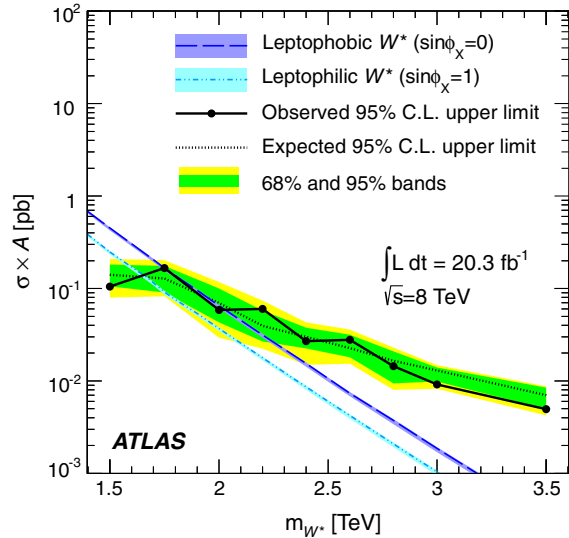


FIG. 6 (color online). Observed (filled circles) and expected 95% C.L. upper limits (dotted line) on $\sigma \times \mathcal{A}$ for leptophobic and nonleptophobic excited vector bosons W^* as a function of particle mass. The green and yellow bands represent the 68% and 95% contours of the expected limit. The dashed curve is the theoretical prediction of $\sigma \times \mathcal{A}$. The uncertainty on the nominal signal cross section due to the beam energy uncertainty is also displayed as a band around the theory prediction. The observed (expected) mass limit occurs at the crossing of the dashed $\sigma \times \mathcal{A}$ curve with the observed (expected) 95% C.L. upper limit curve.

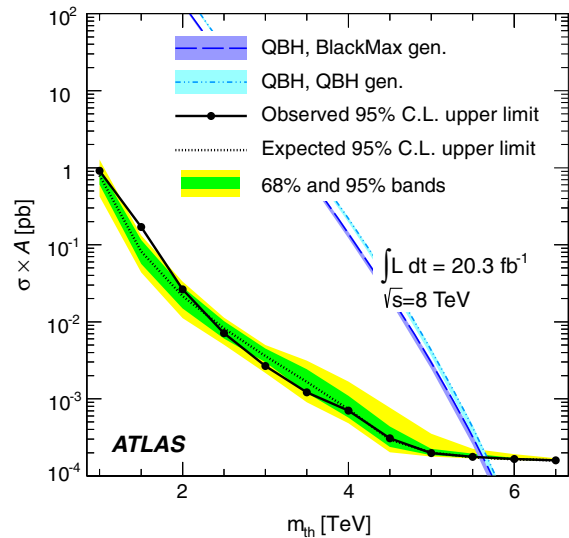


FIG. 7 (color online). Observed (filled circles) and expected 95% C.L. upper limits (dotted line) on $\sigma \times \mathcal{A}$ for black holes simulated using the QBH and BLACKMAX generators as a function of particle mass. The green and yellow bands represent the 68% and 95% contours of the expected limit. The dashed curve is the theoretical prediction of $\sigma \times \mathcal{A}$. The uncertainty on the nominal signal cross section due to the beam energy uncertainty is also displayed as a band around the theory prediction. The observed (expected) mass limit occurs at the crossing of the dashed $\sigma \times \mathcal{A}$ curve with the observed (expected) 95% C.L. upper limit curve.

Exclusion limits on quantum black holes are set starting from 1 TeV in light of the large cross section and of previous exclusion limits [77,80].

C. Generic resonance limits on dijet production

The resulting limits on $\sigma \times \mathcal{A}$ for the Gaussian template shape are shown in Fig. 8. Limits resulting from the convolution of Breit-Wigner signals of different intrinsic widths (Γ_{BW}) with the appropriate parton distribution function, parton shower, nonperturbative effects and detector resolution are shown in Figs. 9 and 10. For the initial Breit-Wigner signal the following nonrelativistic function was chosen:

$$f(x, \mu, \Gamma) = \frac{1}{2\pi} \frac{\Gamma}{(x - \mu)^2 + (\Gamma^2/4)}, \quad (3)$$

where μ and Γ are the mass and the width of the resonance. The use of a relativistic Breit-Wigner signal for the resonance line shape may lead to different limits than the ones derived using the nonrelativistic approximation above. Parton showers and nonperturbative effects have been simulated using HERWIG ++ 2.6.3, which gives a more conservative limit with respect to what is obtained from PYTHIA.

The difference in shapes between the two Breit-Wigner limits is a result of the much larger low-mass tails resulting from the gg parton luminosity, which becomes especially pronounced at high masses. The convolution with parton shower and nonperturbative effects enhances this effect further.

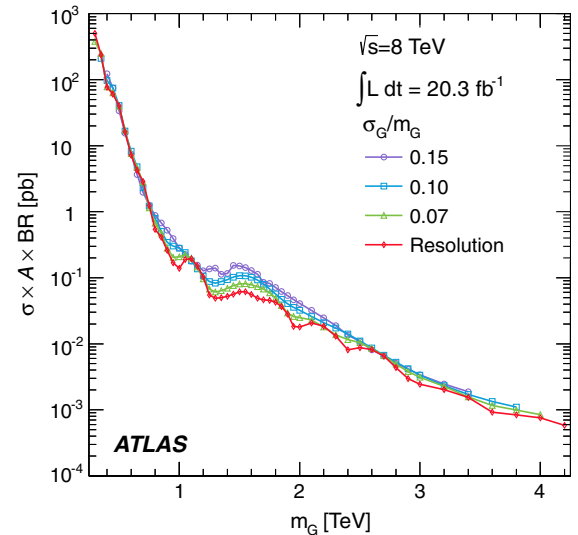


FIG. 8 (color online). The 95% C.L. upper limits on $\sigma \times \mathcal{A}$ for a simple Gaussian resonance decaying to dijets as a function of the mean mass, m_G , for four values of σ_G/m_G , taking into account both statistical and systematic uncertainties.

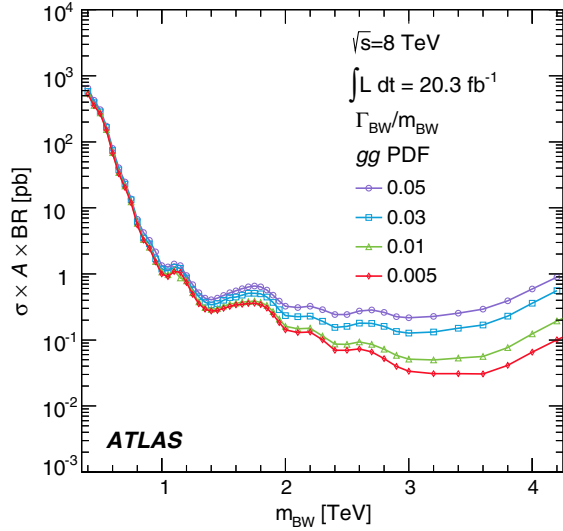


FIG. 9 (color online). The 95% C.L. upper limits on $\sigma \times \mathcal{A}$ for a Breit-Wigner narrow resonance produced by a gg initial state decaying to dijets and convolved with PDF effects, dijet mass acceptance, parton shower and nonperturbative effects and detector resolution, as a function of the mean mass, m_{BW} , for different values of intrinsic width over mass ($\Gamma_{\text{BW}}/m_{\text{BW}}$), taking into account both statistical and systematic uncertainties.

For sufficiently narrow resonances, these results may be used to set limits on NP models beyond those considered in the current studies, as described in detail in Appendix A.

It should be noted that these limits will be conservative at high masses with respect to the limits obtained with full

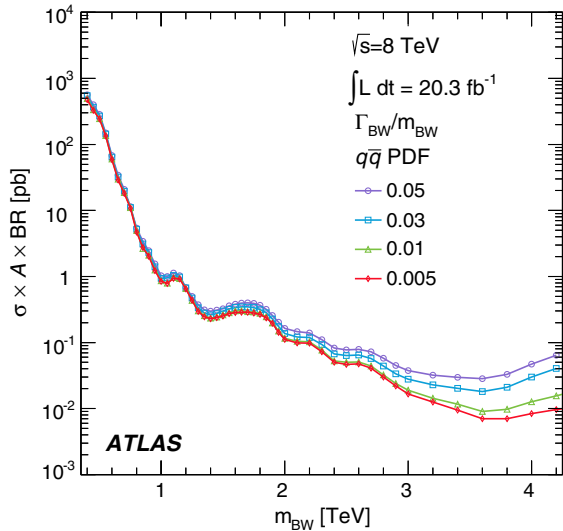


FIG. 10 (color online). The 95% C.L. upper limits on $\sigma \times \mathcal{A}$ for a Breit-Wigner narrow resonance produced by a $q\bar{q}$ initial state decaying to dijets and convolved with PDF effects, dijet mass acceptance, parton shower and nonperturbative effects and detector resolution, as a function of the mean mass, m_{BW} , for different values of intrinsic width over mass ($\Gamma_{\text{BW}}/m_{\text{BW}}$), taking into account both statistical and systematic uncertainties.

benchmark templates. This is due to the simplifying assumptions made in their derivation, in particular from the use of a nonrelativistic and mass-independent Breit-Wigner shape.

Gaussian limits should be used when tails from PDF and nonperturbative effects can be safely truncated or neglected. Otherwise, convolved Breit-Wigner signals would be more reliable.

In the case of the Gaussian limits, the signal distribution after applying the kinematic selection criteria on y^* , m_{jj} and η of the leading jets (Sec. III) should approach a Gaussian distribution. The acceptance should include the jet reconstruction efficiency (100% for the current analysis and detector conditions, since inefficiencies due to calorimeter problems are corrected for in data) and the efficiency with respect to the kinematic selection above. NP models with a width smaller than 5% should be compared to the results with width equal to the experimental resolution only (see Appendix B). For models with a larger width after detector effects, the limit that best matches their width should be used.

VII. CONCLUSIONS

In the 2012 running of the ATLAS experiment at the LHC, the collision energy was raised from 7 TeV to 8 TeV, accompanied by a more than fourfold increase in integrated luminosity. The higher energy, and the associated rise in parton luminosity for high masses, have increased the sensitivity of the search and its mass reach for various model hypotheses. In addition, novel trigger techniques have been employed to extend the search to low dijet masses. The data sample used in the current analysis consists of 20.3 fb^{-1} of pp collision data at $\sqrt{s} = 8 \text{ TeV}$, and the resulting dijet mass distribution extends from 250 GeV to approximately 4.5 TeV.

No resonancelike features are observed in the dijet mass spectrum. This analysis places limits on the cross section times acceptance at the 95% credibility level on the mass or

TABLE I. The 95% C.L. lower limits on the masses and energy scales of the models examined in this study. All limit analyses are Bayesian, with statistical and systematic uncertainties included.

| Model and final state | 95% C.L. limits [TeV] | |
|---|-----------------------|----------|
| | Expected | Observed |
| $q^* \rightarrow qg$ | 3.98 | 4.06 |
| $s_8 \rightarrow gg$ | 2.80 | 2.70 |
| $W' \rightarrow q\bar{q}'$ | 2.51 | 2.45 |
| Leptophobic $W^* \rightarrow q\bar{q}'$ | 1.95 | 1.75 |
| Leptophilic $W^* \rightarrow q\bar{q}'$ | 1.66 | 1.65 |
| QBH black holes | 5.66 | 5.66 |
| (q and g decays only) | | |
| BLACKMAX black holes (all decays) | 5.62 | 5.62 |

TABLE II. ATLAS previous and current expected 95% C.L. upper limits [TeV] on excited quarks and color-octet scalars.

| \sqrt{s} | \mathcal{L} | Citation | q^* [TeV] | $s8$ [TeV] |
|------------|-----------------------|----------|-------------|------------|
| 7 TeV | 36 pb ⁻¹ | [11] | 2.07 | - |
| 7 TeV | 1.0 fb ⁻¹ | [12] | 2.81 | 1.77 |
| 7 TeV | 4.8 fb ⁻¹ | [13] | 2.94 | 1.97 |
| 8 TeV | 20.3 fb ⁻¹ | Current | 3.98 | 2.80 |

energy scale of a variety of hypotheses for physics phenomena beyond the Standard Model.

To illustrate the typical increases in sensitivity to new phenomena at the LHC up to the end of 2012 running, Table II shows the history of expected limits from ATLAS studies using dijet resonance analysis of two benchmark models, excited quarks and color-octet scalars. The limits set by this analysis on excited quarks, color-octet scalars, heavy W' bosons, chiral W^* bosons, and quantum black holes, are summarized in Table I.

ACKNOWLEDGMENTS

We thank CERN for the very successful operation of the LHC, as well as the support staff from our institutions without whom ATLAS could not be operated efficiently. We acknowledge the support of ANPCyT, Argentina; YerPhI, Armenia; ARC, Australia; BMWFW and FWF, Austria; ANAS, Azerbaijan; SSTC, Belarus; CNPq and FAPESP, Brazil; NSERC, NRC and CFI, Canada; CERN; CONICYT, Chile; CAS, MOST and NSFC, China; COLCIENCIAS, Colombia; MSMT CR, MPO CR and VSC CR, Czech Republic; DNRF, DNSRC and Lundbeck Foundation, Denmark; EPLANET, ERC and NSRF, European Union; IN2P3-CNRS, CEA-DSM/IRFU, France; GNSF, Georgia; BMBF, DFG, HGF, MPG and AvH Foundation, Germany; GSRT and NSRF, Greece; ISF, MINERVA, GIF, I-CORE and Benoziyo Center, Israel; INFN, Italy; MEXT and JSPS, Japan; CNRST, Morocco; FOM and NWO, Netherlands; BRF and RCN, Norway; MNiSW and NCN, Poland; GRICES and FCT, Portugal; MNE/IFA, Romania; MES of Russia and ROSATOM, Russian Federation; JINR; MSTD, Serbia; MSSR, Slovakia; ARRS and MIZŠ, Slovenia; DST/NRF, South Africa; MINECO, Spain; SRC and Wallenberg Foundation, Sweden; SER, SNSF and Cantons of Bern and Geneva, Switzerland; NSC, Taiwan; TAEK, Turkey; STFC, the Royal Society and Leverhulme Trust, United Kingdom; DOE and NSF, United States of America. The crucial computing support from all WLCG partners is acknowledged gratefully, in particular from CERN and the ATLAS Tier-1 facilities at TRIUMF (Canada), NDGF (Denmark, Norway, Sweden), CC-IN2P3 (France), KIT/GridKA (Germany), INFN-CNAF (Italy), NL-T1 (Netherlands), PIC (Spain), ASGC (Taiwan), RAL (UK) and BNL (USA) and in the Tier-2 facilities worldwide.

APPENDIX A: SUGGESTED PROCEDURE FOR SETTING LIMITS ON GENERIC NP MODELS

1. Setting limits for NP models with a Gaussian shape

The following detailed procedure is appropriate for setting limits involving resonances that are approximately Gaussian near the core, and with tails that are much smaller than the background. The results of Fig. 8 are provided in tables on HepData.

- (1) Generate an MC sample of a hypothetical new particle with mass set to M . Nonperturbative effects should be included in the event generation. Apply the kinematic selection on the parton η , p_T , and $|y^*|$ used in this analysis, as in Sec. III.
- (2) Smear the signal mass distribution to reflect the detector resolution. The smearing factors derived from full ATLAS simulation of QCD dijet events can be taken from Fig. 11.
- (3) Since a Gaussian signal shape has been assumed in determining the limits, any long tails in the reconstructed m_{jj} should be removed in the sample under study. The recommendation (based on optimization using q^* templates) is to retain events with m_{jj} between $0.8M$ and $1.2M$. The mean mass, m , should be recalculated for this truncated signal.
- (4) The fraction of MC events surviving the first four steps determines the modified acceptance, \mathcal{A} .
- (5) From the table in HepData, select m_G so that $m_G = m$. If the exact value of m is not among the listed values of m_G , check the limit for the two values of m_G that are directly above and below m , and use the larger of the two limits to be conservative.
- (6) To retain enough of the information in the full signal template, and at the same time reject tails that would invalidate the Gaussian approximation, the following truncation procedure is recommended. For

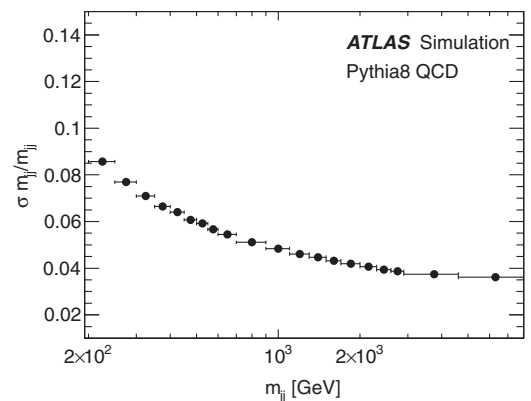


FIG. 11. Dijet mass resolution obtained from fully simulated PYTHIA QCD Monte Carlo PYTHIA 8.175 [43], with the AU2 tune obtained from ATLAS data [45]. The dijet mass resolution is interpolated linearly between the bin centers.

this mass point, choose a value of σ_G/m_G such that the region within $\pm 2\sigma_G$ is well contained in the (truncated) mass range. For the q^* case a good choice is $\sigma_G = (1.2M - 0.8M)/5$ so that 95% of the Gaussian spans $4 \times (0.4/5)M$. Use this value to pick the closest σ_G/m_G value, rounded up to be conservative.

- (7) Compare the tabulated 95% C.L. upper limit corresponding to the chosen m_G and σ_G/m_G values to the $\sigma \times \mathcal{A}$ obtained from the theoretical cross section of the model multiplied by the acceptance defined in step (4) above and taking into account its branching ratio into dijets.

2. Setting limits for NP models with a Breit-Wigner shape, accounting for PDF effects

The following detailed procedure is appropriate for setting limits involving resonances that approximate a Breit-Wigner (BW) shape and extend with a low-mass tail due to effects of parton luminosity. For signals that are very narrow or whose tails deviate significantly from a BW, a truncation of the signal template suggested in the Gaussian limits in Sec. A 1 might be more appropriate. The results of Figs. 9 and 10 are provided in Tables I and II on HepData.

- (1) Generate a hypothetical new particle, with mass set to M and intrinsic width Γ . As the PDF used to obtain those limits is CT10, the same choice is recommended for the event generation. Nonperturbative effects should be simulated after the hard scattering.
- (2) Smear the signal mass distribution to reflect the detector resolution. The smearing factors for the dijet mass are derived from full ATLAS simulation and can be taken from Fig. 11.
- (3) The kinematic selection detailed in Sec. III should be applied to the simulated events. It should be checked at this point that the shape of the template after the $y^* < 0.6$ cut does not change significantly. For example, in a simple model with a flat distribution for the cosine of the polar angle of the jets in the rest frame of the resonance ($\cos\theta^*$) that decays into two back-to-back jets ($y_{\text{lead}} \approx -y_{\text{sublead}}$), a cut on $|y^*| = 0.5 * |y_{\text{lead}} - y_{\text{sublead}}| < 0.6$ imposes a cut on the unboosted rapidity distribution ($|y_{\text{lead,sublead}}| < 0.6$). In the mass ranges investigated, this corresponds to a more stringent constraint than the $\eta_{\text{BW}} < 2.8$ acceptance correction, leading to an acceptance of ~ 0.5 that does not depend on dijet mass. Deviations from a flat acceptance of up to 20% can be observed in the tails of models with different angular distributions (q^* , $s8$, W').

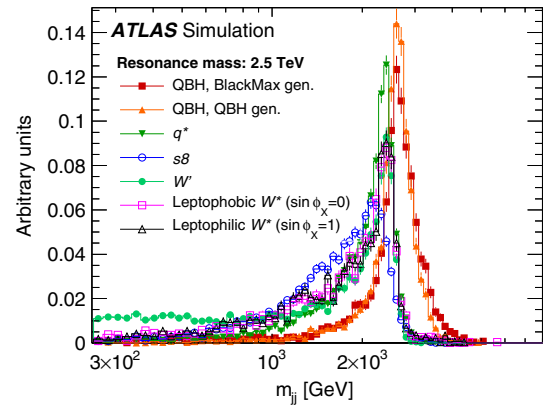


FIG. 12 (color online). Dijet invariant mass for models corresponding to a resonance mass of 2.5 TeV. All distributions are normalized to the same area.

- (4) The fraction of generated events surviving the first three steps determines the signal acceptance, \mathcal{A} .
- (5) From the tables available in HepData, select the one corresponding to the production mode for the new resonance (gluon-gluon, gluon-quark, quark-quark or quark-antiquark) as the parton luminosities and hence the signal shapes differ.
- (6) Compare the tabulated 95% C.L. upper limit corresponding to the chosen M and Γ/M values to the $\sigma \times \mathcal{A}$ obtained from the theoretical cross section of the model, multiplied by the acceptance defined in step (3) above and taking into account its branching ratio into dijets.

If the exact values of M and Γ/M are not among the listed values of m_{BW} and $\Gamma_{\text{BW}}/m_{\text{BW}}$, check the limit for the two values of m_{BW} that are directly above and below M , and use the more conservative of the two limits.

APPENDIX B: DIJET MASS RESOLUTION

The dijet mass resolution in Fig. 11 is derived from fully simulated QCD Monte Carlo, generated with PYTHIA 8.175 [43], using the AU2 tune obtained from ATLAS data [45] using the analysis selection detailed in Sec. III. The dijet mass resolution $\sigma_{m_{jj}}/m_{jj}$ is 8% at $m_{jj} \approx 250$ GeV falls to 4% at 2 TeV and approaches 4% at m_{jj} of 3 TeV and above, and it is interpolated linearly between the bin centers.

APPENDIX C: SIGNAL TEMPLATE SHAPES

For ease of comparison of the shapes of different signals used in this paper, the various signal template shapes are overlaid in Fig. 12 for the mass point of 2.5 TeV, after normalizing to the same area.

- [1] G. Arnison *et al.* (UA1 Collaboration), *Phys. Lett.* **136B**, 294 (1984).
- [2] P. Bagnaia *et al.* (UA2 Collaboration), *Phys. Lett.* **144B**, 283 (1984).
- [3] T. Aaltonen *et al.* (CDF Collaboration), *Phys. Rev. D* **79**, 112002 (2009).
- [4] V. Abazov *et al.* (D0 Collaboration), *Phys. Rev. Lett.* **103**, 191803 (2009).
- [5] ATLAS Collaboration, *Phys. Rev. Lett.* **105**, 161801 (2010).
- [6] ATLAS Collaboration, *Phys. Lett. B* **694**, 327 (2011).
- [7] CMS Collaboration, *Phys. Rev. Lett.* **105**, 211801 (2010).
- [8] CMS Collaboration, *Phys. Rev. Lett.* **105**, 262001 (2010).
- [9] CMS Collaboration, *Phys. Rev. Lett.* **106**, 201804 (2011).
- [10] CMS Collaboration, *Phys. Lett. B* **704**, 123 (2011).
- [11] ATLAS Collaboration, *New J. Phys.* **13**, 053044 (2011).
- [12] ATLAS Collaboration, *Phys. Lett. B* **708**, 37 (2012).
- [13] ATLAS Collaboration, *J. High Energy Phys.* **01** (2013) 029.
- [14] CMS Collaboration, *Phys. Rev. D* **87**, 114015 (2013).
- [15] ATLAS Collaboration, *Eur. Phys. J. C* **73**, 2518 (2013).
- [16] U. Baur, I. Hinchliffe, and D. Zeppenfeld, *Int. J. Mod. Phys. A* **02**, 1285 (1987).
- [17] U. Baur, M. Spira, and P. M. Zerwas, *Phys. Rev. D* **42**, 815 (1990).
- [18] P. H. Frampton and S. L. Glashow, *Phys. Lett. B* **190**, 157 (1987).
- [19] P. H. Frampton and S. L. Glashow, *Phys. Rev. Lett.* **58**, 2168 (1987).
- [20] J. Bagger, C. Schmidt, and S. King, *Phys. Rev. D* **37**, 1188 (1988).
- [21] T. Han, I. Lewis, and Z. Liu, *J. High Energy Phys.* **12** (2010) 085.
- [22] H. Georgi, E. E. Jenkins, and E. H. Simmons, *Nucl. Phys.* **B331**, 541 (1990).
- [23] C. Grojean, E. Salvioni, and R. Torre, *J. High Energy Phys.* **07** (2011) 002.
- [24] M. Cvetič and J. C. Pati, *Phys. Lett.* **135B**, 57 (1984).
- [25] Y. Mimura and S. Nandi, *Phys. Lett. B* **538**, 406 (2002).
- [26] G. Altarelli, B. Mele, and M. Ruiz-Altaba, *Z. Phys. C* **45**, 109 (1989).
- [27] G. Altarelli, B. Mele, and M. Ruiz-Altaba, *Z. Phys. C* **47**, 676 (1990).
- [28] CMS Collaboration, *Phys. Lett. B* **701**, 160 (2011).
- [29] ATLAS Collaboration, *Phys. Lett. B* **705**, 28 (2011).
- [30] M. Chizhov, *Phys. Part. Nucl. Lett.* **8**, 512 (2011).
- [31] M. Chizhov and G. Dvali, *Phys. Lett. B* **703**, 593 (2011).
- [32] M. Chizhov, V. Bednyakov, and J. Budagov, *Phys. At. Nucl.* **75**, 90 (2012).
- [33] M. Chizhov, V. Bednyakov, and J. Budagov, [arXiv:1106.4161](https://arxiv.org/abs/1106.4161).
- [34] L. A. Anchordoqui, J. L. Feng, H. Goldberg, and A. D. Shapere, *Phys. Lett. B* **594**, 363 (2004).
- [35] P. Meade and L. Randall, *J. High Energy Phys.* **05** (2008) 003.
- [36] X. Calmet, W. Gong, and S. D. Hsu, *Phys. Lett. B* **668**, 20 (2008).
- [37] D. M. Gingrich, *J. Phys. G* **37**, 105008 (2010).
- [38] ATLAS Collaboration, *JINST* **3**, S08003 (2008).
- [39] W. Lampl *et al.*, Report No. ATL-LARG-PUB-2008-002, 2010, <http://cdsweb.cern.ch/record/1099735>.
- [40] M. Cacciari, G. P. Salam, and G. Soyez, *J. High Energy Phys.* **04** (2008) 063.
- [41] M. Cacciari and G. P. Salam, *Phys. Lett. B* **641**, 57 (2006).
- [42] ATLAS Collaboration, Report No. ATLAS-CONF-2013-083, 2013, <http://cdsweb.cern.ch/record/1570994>.
- [43] T. Sjostrand, S. Mrenna, and P. Z. Skands, *Comput. Phys. Commun.* **178**, 852 (2008).
- [44] H.-L. Lai, M. Guzzi, J. Huston, Z. Li, P. M. Nadolsky, J. Pumplin, and C.-P. Yuan, *Phys. Rev. D* **82**, 074024 (2010).
- [45] ATLAS Collaboration, Report No. ATLAS-PUB-2012-003, 2013, <http://cdsweb.cern.ch/record/1363300>.
- [46] S. Agostinelli *et al.* (GEANT4), *Nucl. Instrum. Methods Phys. Res., Sect. A* **506**, 250 (2003).
- [47] ATLAS Collaboration, *Eur. Phys. J. C* **70**, 823 (2010).
- [48] ATLAS Collaboration, *Eur. Phys. J. C* **75**, 1 (2015).
- [49] ATLAS Collaboration, *Eur. Phys. J. C* **73**, 2306 (2013).
- [50] ATLAS Collaboration, *Eur. Phys. J. C* **72**, 1849 (2012).
- [51] V. Lendermann, J. Haller, M. Herbst, K. Krüger, H.-C. Schultz-Coulon, and R. Stamen, *Nucl. Instrum. Methods Phys. Res., Sect. A* **604**, 707 (2009).
- [52] ATLAS Collaboration, Report No. ATLAS-CONF-2012-020, 2012, <http://cdsweb.cern.ch/record/1430034>.
- [53] ATLAS Collaboration, Report No. ATLAS-CONF-2010-054, 2010, <http://cdsweb.cern.ch/record/1281311>.
- [54] R. M. Harris and K. Kousouris, *Int. J. Mod. Phys. A* **26**, 5005 (2011).
- [55] ATLAS Collaboration, CERN, 2012, Report No. ATLAS-CONF-2012-148.
- [56] Z. Nagy, *Phys. Rev. Lett.* **88**, 122003 (2002).
- [57] S. Catani and M. H. Seymour, *Nucl. Phys.* **B485**, 291 (1997); **B510**, 503 (1998).
- [58] G. Choudalakis and D. Casadei, *Eur. Phys. J. Plus* **127**, 25 (2012).
- [59] T. Aaltonen *et al.* (CDF Collaboration), *Phys. Rev. D* **79**, 011101 (2009).
- [60] G. Choudalakis, [arXiv:1101.0390](https://arxiv.org/abs/1101.0390).
- [61] L. Lyons, *Ann. Appl. Stat.* **2**, 887 (2008).
- [62] R. Corke and T. Sjostrand, *Eur. Phys. J. C* **69**, 1 (2010).
- [63] T. Sjostrand and P. Z. Skands, *Eur. Phys. J. C* **39**, 129 (2005).
- [64] B. Andersson, G. Gustafson, G. Ingelman, and T. Sjostrand, *Phys. Rep.* **97**, 31 (1983).
- [65] J. Alwall, M. Herquet, F. Maltoni, O. Mattelaer, and T. Stelzer, *J. High Energy Phys.* **06** (2011) 128.
- [66] A. Martin, W. Stirling, R. Thorne, and G. Watt, *Eur. Phys. J. C* **63**, 189 (2009).
- [67] ATLAS Collaboration, *J. High Energy Phys.* **09** (2014) 037.
- [68] D.-C. Dai, G. Starkman, D. Stojkovic, C. Issever, E. Rizvi, and J. Tseng, *Phys. Rev. D* **77**, 076007 (2008).
- [69] D. M. Gingrich, *Comput. Phys. Commun.* **181**, 1917 (2010).
- [70] N. Arkani-Hamed, S. Dimopoulos, and G. Dvali, *Phys. Rev. D* **59**, 086004 (1999).
- [71] hepdata repository for results in this paper: <http://hepdata.cedar.ac.uk/view/red6339>
- [72] ATLAS Collaboration, Report No. ATL-PHYS-PUB-2010-013, 2010, <http://cdsweb.cern.ch/record/1300517>.
- [73] A. Caldwell, D. Kollár, and K. Kröninger, *Comput. Phys. Commun.* **180**, 2197 (2009).

- [74] G. Corcella, I. G. Knowles, G. Marchesini, S. Moretti, K. Odagiri, P. Richardson, M. H. Seymour, and B. R. Webber, *J. High Energy Phys.* **01** (2001) 010.
- [75] G. Marchesini, B. R. Webber, G. Abbiendi, I. G. Knowles, M. H. Seymour, and L. Stanco, *Comput. Phys. Commun.* **67**, 465 (1992).
- [76] R. Kohavi, *IJCAI* **14**, 1137 (1995).
- [77] ATLAS Collaboration, *Phys. Lett. B* **728**, 562 (2014).
- [78] M. Botje *et al.*, [arXiv:1101.0538](https://arxiv.org/abs/1101.0538).
- [79] R. D. Ball, V. Bertone, F. Cerutti, L. Del Debbio, S. Forte, A. Guffanti, J. I. Latorre, J. Rojo, and M. Ubiali, *Nucl. Phys.* **B849**, 296 (2011).
- [80] ATLAS Collaboration, *Phys. Rev. Lett.* **112**, 091804 (2014).

G. Aad,⁸⁴ B. Abbott,¹¹² J. Abdallah,¹⁵² S. Abdel Khalek,¹¹⁶ O. Abdinov,¹¹ R. Aben,¹⁰⁶ B. Abi,¹¹³ M. Abolins,⁸⁹ O. S. AbouZeid,¹⁵⁹ H. Abramowicz,¹⁵⁴ H. Abreu,¹⁵³ R. Abreu,³⁰ Y. Abulaiti,^{147a,147b} B. S. Acharya,^{165a,165b,b} L. Adamczyk,^{38a} D. L. Adams,²⁵ J. Adelman,¹⁷⁷ S. Adomeit,⁹⁹ T. Adye,¹³⁰ T. Agatonovic-Jovin,^{13a} J. A. Aguilar-Saavedra,^{125a,125f} M. Agustoni,¹⁷ S. P. Ahlen,²² F. Ahmadov,^{64,c} G. Aielli,^{134a,134b} H. Akerstedt,^{147a,147b} T. P. A. Åkesson,⁸⁰ G. Akimoto,¹⁵⁶ A. V. Akimov,⁹⁵ G. L. Alberghi,^{20a,20b} J. Albert,¹⁷⁰ S. Albrand,⁵⁵ M. J. Alconada Verzini,⁷⁰ M. Aleksa,³⁰ I. N. Aleksandrov,⁶⁴ C. Alexa,^{26a} G. Alexander,¹⁵⁴ G. Alexandre,⁴⁹ T. Alexopoulos,¹⁰ M. Alhroob,^{165a,165c} G. Alimonti,^{90a} L. Alio,⁸⁴ J. Alison,³¹ B. M. M. Allbrooke,¹⁸ L. J. Allison,⁷¹ P. P. Allport,⁷³ J. Almond,⁸³ A. Aloisio,^{103a,103b} A. Alonso,³⁶ F. Alonso,⁷⁰ C. Alpigiani,⁷⁵ A. Altheimer,³⁵ B. Alvarez Gonzalez,⁸⁹ M. G. Alviggi,^{103a,103b} K. Amako,⁶⁵ Y. Amaral Coutinho,^{24a} C. Amelung,²³ D. Amidei,⁸⁸ S. P. Amor Dos Santos,^{125a,125c} A. Amorim,^{125a,125b} S. Amoroso,⁴⁸ N. Amram,¹⁵⁴ G. Amundsen,²³ C. Anastopoulos,¹⁴⁰ L. S. Ancu,⁴⁹ N. Andari,³⁰ T. Andeen,³⁵ C. F. Anders,^{58b} G. Anders,³⁰ K. J. Anderson,³¹ A. Andreazza,^{90a,90b} V. Andrei,^{58a} X. S. Anduaga,⁷⁰ S. Angelidakis,⁹ I. Angelozzi,¹⁰⁶ P. Anger,⁴⁴ A. Angerami,³⁵ F. Anghinolfi,³⁰ A. V. Anisenkov,¹⁰⁸ N. Anjos,^{125a} A. Annovi,⁴⁷ A. Antonaki,⁹ M. Antonelli,⁴⁷ A. Antonov,⁹⁷ J. Antos,^{145b} F. Anulli,^{133a} M. Aoki,⁶⁵ L. Aperio Bella,¹⁸ R. Apolle,^{119,d} G. Arabidze,⁸⁹ I. Aracena,¹⁴⁴ Y. Arai,⁶⁵ J. P. Araque,^{125a} A. T. H. Arce,⁴⁵ J-F. Arguin,⁹⁴ S. Argyropoulos,⁴² M. Arik,^{19a} A. J. Armbruster,³⁰ O. Arnaez,³⁰ V. Arnal,⁸¹ H. Arnold,⁴⁸ M. Arratia,²⁸ O. Arslan,²¹ A. Artamonov,⁹⁶ G. Artoni,²³ S. Asai,¹⁵⁶ N. Asbah,⁴² A. Ashkenazi,¹⁵⁴ B. Åsman,^{147a,147b} L. Asquith,⁶ K. Assamagan,²⁵ R. Astalos,^{145a} M. Atkinson,¹⁶⁶ N. B. Atlay,¹⁴² B. Auerbach,⁶ K. Augsten,¹²⁷ M. Aurousseau,^{146b} G. Avolio,³⁰ G. Azuelos,^{94,e} Y. Azuma,¹⁵⁶ M. A. Baak,³⁰ A. Baas,^{58a} C. Bacci,^{135a,135b} H. Bachacou,¹³⁷ K. Bachas,¹⁵⁵ M. Backes,³⁰ M. Backhaus,³⁰ J. Backus Mayes,¹⁴⁴ E. Badescu,^{26a} P. Bagiacchi,^{133a,133b} P. Bagnaia,^{133a,133b} Y. Bai,^{33a} T. Bain,³⁵ J. T. Baines,¹³⁰ O. K. Baker,¹⁷⁷ P. Balek,¹²⁸ F. Balli,¹³⁷ E. Banas,³⁹ Sw. Banerjee,¹⁷⁴ A. A. E. Bannoura,¹⁷⁶ V. Bansal,¹⁷⁰ H. S. Bansil,¹⁸ L. Barak,¹⁷³ S. P. Baranov,⁹⁵ E. L. Barberio,⁸⁷ D. Barberis,^{50a,50b} M. Barbero,⁸⁴ T. Barillari,¹⁰⁰ M. Barisonzi,¹⁷⁶ T. Barklow,¹⁴⁴ N. Barlow,²⁸ B. M. Barnett,¹³⁰ R. M. Barnett,¹⁵ Z. Barnovska,⁵ A. Baroncelli,^{135a} G. Barone,⁴⁹ A. J. Barr,¹¹⁹ F. Barreiro,⁸¹ J. Barreiro Guimarães da Costa,⁵⁷ R. Bartoldus,¹⁴⁴ A. E. Barton,⁷¹ P. Bartos,^{145a} V. Bartsch,¹⁵⁰ A. Bassalat,¹¹⁶ A. Basye,¹⁶⁶ R. L. Bates,⁵³ J. R. Batley,²⁸ M. Battaglia,¹³⁸ M. Battistin,³⁰ F. Bauer,¹³⁷ H. S. Bawa,^{144,f} M. D. Beattie,⁷¹ T. Beau,⁷⁹ P. H. Beauchemin,¹⁶² R. Beccherle,^{123a,123b} P. Bechtel,²¹ H. P. Beck,¹⁷ K. Becker,¹⁷⁶ S. Becker,⁹⁹ M. Beckingham,¹⁷¹ C. Becot,¹¹⁶ A. J. Beddall,^{19c} A. Beddall,^{19c} S. Bedikian,¹⁷⁷ V. A. Bednyakov,⁶⁴ C. P. Bee,¹⁴⁹ L. J. Beamster,¹⁰⁶ T. A. Beermann,¹⁷⁶ M. Begel,²⁵ K. Behr,¹¹⁹ C. Belanger-Champagne,⁸⁶ P. J. Bell,⁴⁹ W. H. Bell,⁴⁹ G. Bella,¹⁵⁴ L. Bellagamba,^{20a} A. Bellerive,²⁹ M. Bellomo,⁸⁵ K. Belotskiy,⁹⁷ O. Beltramello,³⁰ O. Benary,¹⁵⁴ D. Bencheikroun,^{136a} K. Bendtz,^{147a,147b} N. Benekos,¹⁶⁶ Y. Benhammou,¹⁵⁴ E. Benhar Noccioli,⁴⁹ J. A. Benitez Garcia,^{160b} D. P. Benjamin,⁴⁵ J. R. Bensinger,²³ K. Benslama,¹³¹ S. Bentvelsen,¹⁰⁶ D. Berge,¹⁰⁶ E. Bergeaas Kuutmann,¹⁶ N. Berger,⁵ F. Berghaus,¹⁷⁰ J. Beringer,¹⁵ C. Bernard,²² P. Bernat,⁷⁷ C. Bernius,⁷⁸ F. U. Bernlochner,¹⁷⁰ T. Berry,⁷⁶ P. Berta,¹²⁸ C. Bertella,⁸⁴ G. Bertoli,^{147a,147b} F. Bertolucci,^{123a,123b} C. Bertsche,¹¹² D. Bertsche,¹¹² M. I. Besana,^{90a} G. J. Besjes,¹⁰⁵ O. Bessidskaia Bylund,^{147a,147b} M. Bessner,⁴² N. Besson,¹³⁷ C. Betancourt,⁴⁸ S. Bethke,¹⁰⁰ W. Bhimji,⁴⁶ R. M. Bianchi,¹²⁴ L. Bianchini,²³ M. Bianco,³⁰ O. Biebel,⁹⁹ S. P. Bieniek,⁷⁷ K. Bierwagen,⁵⁴ J. Biesiada,¹⁵ M. Biglietti,^{135a} J. Bilbao De Mendizabal,⁴⁹ H. Bilokon,⁴⁷ M. Bindi,⁵⁴ S. Binet,¹¹⁶ A. Bingul,^{19c} C. Bini,^{133a,133b} C. W. Black,¹⁵¹ J. E. Black,¹⁴⁴ K. M. Black,²² D. Blackburn,¹³⁹ R. E. Blair,⁶ J.-B. Blanchard,¹³⁷ T. Blazek,^{145a} I. Bloch,⁴² C. Blocker,²³ W. Blum,^{82,a} U. Blumenschein,⁵⁴ G. J. Bobbink,¹⁰⁶ V. S. Bobrovnikov,¹⁰⁸ S. S. Bocchetta,⁸⁰ A. Bocci,⁴⁵ C. Bock,⁹⁹ C. R. Boddy,¹¹⁹ M. Boehler,⁴⁸ T. T. Boek,¹⁷⁶ J. A. Bogaerts,³⁰ A. G. Bogdanchikov,¹⁰⁸ A. Bogouch,^{91,a} C. Bohm,^{147a} J. Bohm,¹²⁶ V. Boisvert,⁷⁶ T. Bold,^{38a} V. Boldea,^{26a} A. S. Boldyrev,⁹⁸ M. Bomben,⁷⁹ M. Bona,⁷⁵ M. Boonekamp,¹³⁷ A. Borisov,¹²⁹ G. Borissov,⁷¹ M. Borri,⁸³ S. Borroni,⁴² J. Bortfeldt,⁹⁹ V. Bortolotto,^{135a,135b} K. Bos,¹⁰⁶ D. Boscherini,^{20a} M. Bosman,¹² H. Boterenbrood,¹⁰⁶ J. Boudreau,¹²⁴ J. Bouffard,² E. V. Bouhova-Thacker,⁷¹

D. Boumediene,³⁴ C. Bourdarios,¹¹⁶ N. Bousson,¹¹³ S. Boutouil,^{136d} A. Boveia,³¹ J. Boyd,³⁰ I. R. Boyko,⁶⁴ J. Bracinik,¹⁸ A. Brandt,⁸ G. Brandt,¹⁵ O. Brandt,^{58a} U. Bratzler,¹⁵⁷ B. Brau,⁸⁵ J. E. Brau,¹¹⁵ H. M. Braun,^{176,a} S. F. Brazzale,^{165a,165c} B. Brelrier,¹⁵⁹ K. Brendlinger,¹²¹ A. J. Brennan,⁸⁷ R. Brenner,¹⁶⁷ S. Bressler,¹⁷³ K. Bristow,^{146c} T. M. Bristow,⁴⁶ D. Britton,⁵³ F. M. Brochu,²⁸ I. Brock,²¹ R. Brock,⁸⁹ C. Bromberg,⁸⁹ J. Bronner,¹⁰⁰ G. Brooijmans,³⁵ T. Brooks,⁷⁶ W. K. Brooks,^{32b} J. Brosamer,¹⁵ E. Brost,¹¹⁵ J. Brown,⁵⁵ P. A. Bruckman de Renstrom,³⁹ D. Bruncko,^{145b} R. Bruneliere,⁴⁸ S. Brunet,⁶⁰ A. Bruni,^{20a} G. Bruni,^{20a} M. Bruschi,^{20a} L. Bryngemark,⁸⁰ T. Buanes,¹⁴ Q. Buat,¹⁴³ F. Bucci,⁴⁹ P. Buchholz,¹⁴² R. M. Buckingham,¹¹⁹ A. G. Buckley,⁵³ S. I. Buda,^{26a} I. A. Budagov,⁶⁴ F. Buehrer,⁴⁸ L. Bugge,¹¹⁸ M. K. Bugge,¹¹⁸ O. Bulekov,⁹⁷ A. C. Bundock,⁷³ H. Burckhart,³⁰ S. Burdin,⁷³ B. Burghgrave,¹⁰⁷ S. Burke,¹³⁰ I. Burmeister,⁴³ E. Busato,³⁴ D. Büscher,⁴⁸ V. Büscher,⁸² P. Bussey,⁵³ C. P. Buszello,¹⁶⁷ B. Butler,⁵⁷ J. M. Butler,²² A. I. Butt,³ C. M. Buttar,⁵³ J. M. Butterworth,⁷⁷ P. Butti,¹⁰⁶ W. Buttinger,²⁸ A. Buzatu,⁵³ M. Byszewski,¹⁰ S. Cabrera Urbán,¹⁶⁸ D. Caforio,^{20a,20b} O. Cakir,^{4a} P. Calafiura,¹⁵ A. Calandri,¹³⁷ G. Calderini,⁷⁹ P. Calfayan,⁹⁹ R. Calkins,¹⁰⁷ L. P. Caloba,^{24a} D. Calvet,³⁴ S. Calvet,³⁴ R. Camacho Toro,⁴⁹ S. Camarda,⁴² D. Cameron,¹¹⁸ L. M. Caminada,¹⁵ R. Caminal Armadans,¹² S. Campana,³⁰ M. Campanelli,⁷⁷ A. Campoverde,¹⁴⁹ V. Canale,^{103a,103b} A. Canepa,^{160a} M. Cano Bret,⁷⁵ J. Cantero,⁸¹ R. Cantrill,^{125a} T. Cao,⁴⁰ M. D. M. Capeans Garrido,³⁰ I. Caprini,^{26a} M. Caprini,^{26a} M. Capua,^{37a,37b} R. Caputo,⁸² R. Cardarelli,^{134a} T. Carli,³⁰ G. Carlino,^{103a} L. Carminati,^{90a,90b} S. Caron,¹⁰⁵ E. Carquin,^{32a} G. D. Carrillo-Montoya,^{146c} J. R. Carter,²⁸ J. Carvalho,^{125a,125c} D. Casadei,⁷⁷ M. P. Casado,¹² M. Casolino,¹² E. Castaneda-Miranda,^{146b} A. Castelli,¹⁰⁶ V. Castillo Gimenez,¹⁶⁸ N. F. Castro,^{125a} P. Catastini,⁵⁷ A. Catinaccio,³⁰ J. R. Catmore,¹¹⁸ A. Cattai,³⁰ G. Cattani,^{134a,134b} V. Cavaliere,¹⁶⁶ D. Cavalli,^{90a} M. Cavalli-Sforza,¹² V. Cavasinni,^{123a,123b} F. Ceradini,^{135a,135b} B. Cerio,⁴⁵ K. Cerny,¹²⁸ A. S. Cerqueira,^{24b} A. Cerri,¹⁵⁰ L. Cerrito,⁷⁵ F. Cerutti,¹⁵ M. Cerv,³⁰ A. Cervelli,¹⁷ S. A. Cetin,^{19b} A. Chafaq,^{136a} D. Chakraborty,¹⁰⁷ I. Chalupkova,¹²⁸ P. Chang,¹⁶⁶ B. Chapleau,⁸⁶ J. D. Chapman,²⁸ D. Charfeddine,¹¹⁶ D. G. Charlton,¹⁸ C. C. Chau,¹⁵⁹ C. A. Chavez Barajas,¹⁵⁰ S. Cheatham,⁸⁶ A. Chegwiddden,⁸⁹ S. Chekanov,⁶ S. V. Chekulaev,^{160a} G. A. Chelkov,^{64,g} M. A. Chelstowska,⁸⁸ C. Chen,⁶³ H. Chen,²⁵ K. Chen,¹⁴⁹ L. Chen,^{33d,h} S. Chen,^{33c} X. Chen,^{146c} Y. Chen,⁶⁶ Y. Chen,³⁵ H. C. Cheng,⁸⁸ Y. Cheng,³¹ A. Cheplakov,⁶⁴ R. Cherkaoui El Moursli,^{136e} V. Chernyatin,^{25a} E. Cheu,⁷ L. Chevalier,¹³⁷ V. Chiarella,⁴⁷ G. Chiefari,^{103a,103b} J. T. Childers,⁶ A. Chilingarov,⁷¹ G. Chiodini,^{72a} A. S. Chisholm,¹⁸ R. T. Chislett,⁷⁷ A. Chitan,^{26a} M. V. Chizhov,⁶⁴ S. Chouridou,⁹ B. K. B. Chow,⁹⁹ D. Chromek-Burckhart,³⁰ M. L. Chu,¹⁵² J. Chudoba,¹²⁶ J. J. Chwastowski,³⁹ L. Chytka,¹¹⁴ G. Ciapetti,^{133a,133b} A. K. Ciftci,^{4a} R. Ciftci,^{4a} D. Cinca,⁵³ V. Cindro,⁷⁴ A. Ciocio,¹⁵ P. Cirkovic,^{13b} Z. H. Citron,¹⁷³ M. Citterio,^{90a} M. Ciubancan,^{26a} A. Clark,⁴⁹ P. J. Clark,⁴⁶ R. N. Clarke,¹⁵ W. Cleland,¹²⁴ J. C. Clemens,⁸⁴ C. Clement,^{147a,147b} Y. Coadou,⁸⁴ M. Cobal,^{165a,165c} A. Coccaro,¹³⁹ J. Cochran,⁶³ L. Coffey,²³ J. G. Cogan,¹⁴⁴ J. Coggeshall,¹⁶⁶ B. Cole,³⁵ S. Cole,¹⁰⁷ A. P. Colijn,¹⁰⁶ J. Collot,⁵⁵ T. Colombo,^{58c} G. Colon,⁸⁵ G. Compostella,¹⁰⁰ P. Conde Muño,^{125a,125b} E. Coniavitis,⁴⁸ M. C. Conidi,¹² S. H. Connell,^{146b} I. A. Connelly,⁷⁶ S. M. Consonni,^{90a,90b} V. Consorti,⁴⁸ S. Constantinescu,^{26a} C. Conta,^{120a,120b} G. Conti,⁵⁷ F. Conventi,^{103a,i} M. Cooke,¹⁵ B. D. Cooper,⁷⁷ A. M. Cooper-Sarkar,¹¹⁹ N. J. Cooper-Smith,⁷⁶ K. Copic,¹⁵ T. Cornelissen,¹⁷⁶ M. Corradi,^{20a} F. Corriveau,^{86j} A. Corso-Radu,¹⁶⁴ A. Cortes-Gonzalez,¹² G. Cortiana,¹⁰⁰ G. Costa,^{90a} M. J. Costa,¹⁶⁸ D. Costanzo,¹⁴⁰ D. Côté,⁸ G. Cottin,²⁸ G. Cowan,⁷⁶ B. E. Cox,⁸³ K. Cranmer,¹⁰⁹ G. Cree,²⁹ S. Crépe-Renaudin,⁵⁵ F. Crescioli,⁷⁹ W. A. Cribbs,^{147a,147b} M. Crispin Ortuzar,¹¹⁹ M. Cristinziani,²¹ V. Croft,¹⁰⁵ G. Crosetti,^{37a,37b} C.-M. Cuciuc,^{26a} T. Cuhadar Donszelmann,¹⁴⁰ J. Cummings,¹⁷⁷ M. Curatolo,⁴⁷ C. Cuthbert,¹⁵¹ H. Czirr,¹⁴² P. Czodrowski,³ Z. Czynzula,¹⁷⁷ S. D'Auria,⁵³ M. D'Onofrio,⁷³ M. J. Da Cunha Sargedas De Sousa,^{125a,125b} C. Da Via,⁸³ W. Dabrowski,^{38a} A. Dafinca,¹¹⁹ T. Dai,⁸⁸ O. Dale,¹⁴ F. Dallaire,⁹⁴ C. Dallapiccola,⁸⁵ M. Dam,³⁶ A. C. Daniells,¹⁸ M. Dano Hoffmann,¹³⁷ V. Dao,⁴⁸ G. Darbo,^{50a} S. Darmora,⁸ J. A. Dassoulas,⁴² A. Dattagupta,⁶⁰ W. Davey,²¹ C. David,¹⁷⁰ T. Davidek,¹²⁸ E. Davies,^{119,d} M. Davies,¹⁵⁴ O. Davignon,⁷⁹ A. R. Davison,⁷⁷ P. Davison,⁷⁷ Y. Davygora,^{58a} E. Dawe,¹⁴³ I. Dawson,¹⁴⁰ R. K. Daya-Ishmukhametova,⁸⁵ K. De,⁸ R. de Asmundis,^{103a} S. De Castro,^{20a,20b} S. De Cecco,⁷⁹ N. De Groot,¹⁰⁵ P. de Jong,¹⁰⁶ H. De la Torre,⁸¹ F. De Lorenzi,⁶³ L. De Nooij,¹⁰⁶ D. De Pedis,^{133a} A. De Salvo,^{133a} U. De Sanctis,¹⁵⁰ A. De Santo,¹⁵⁰ J. B. De Vivie De Regie,¹¹⁶ W. J. Dearnaley,⁷¹ R. Debbe,²⁵ C. Debenedetti,¹³⁸ B. Dechenaux,⁵⁵ D. V. Dedovich,⁶⁴ I. Deigaard,¹⁰⁶ J. Del Peso,⁸¹ T. Del Prete,^{123a,123b} F. Deliot,¹³⁷ C. M. Delitzsch,⁴⁹ M. Deliyergiyev,⁷⁴ A. Dell'Acqua,³⁰ L. Dell'Asta,²² M. Dell'Orso,^{123a,123b} M. Della Pietra,^{103a,i} D. della Volpe,⁴⁹ M. Delmastro,⁵ P. A. Delsart,⁵⁵ C. Deluca,¹⁰⁶ S. Demers,¹⁷⁷ M. Demichev,⁶⁴ A. Demilly,⁷⁹ S. P. Denisov,¹²⁹ D. Derendarz,³⁹ J. E. Derkaoui,^{136d} F. Derue,⁷⁹ P. Dervan,⁷³ K. Desch,²¹ C. Deterre,⁴² P. O. Deviveiros,¹⁰⁶ A. Dewhurst,¹³⁰ S. Dhaliwal,¹⁰⁶ A. Di Ciaccio,^{134a,134b} L. Di Ciaccio,⁵ A. Di Domenico,^{133a,133b} C. Di Donato,^{103a,103b} A. Di Girolamo,³⁰ B. Di Girolamo,³⁰ A. Di Mattia,¹⁵³ B. Di Micco,^{135a,135b} R. Di Nardo,⁴⁷ A. Di Simone,⁴⁸ R. Di Sipio,^{20a,20b} D. Di Valentino,²⁹ F. A. Dias,⁴⁶ M. A. Diaz,^{32a}

E. B. Diehl,⁸⁸ J. Dietrich,⁴² T. A. Dietzsch,^{58a} S. Diglio,⁸⁴ A. Dimitrievska,^{13a} J. Dingfelder,²¹ C. Dionisi,^{133a,133b} P. Dita,^{26a} S. Dita,^{26a} F. Dittus,³⁰ F. Djama,⁸⁴ T. Djobava,^{51b} M. A. B. do Vale,^{24c} A. Do Valle Wemans,^{125a,125g} D. Dobos,³⁰ C. Doglioni,⁴⁹ T. Doherty,⁵³ T. Dohmae,¹⁵⁶ J. Dolejsi,¹²⁸ Z. Dolezal,¹²⁸ B. A. Dolgoshein,^{97,a} M. Donadelli,^{24d} S. Donati,^{123a,123b} P. Dondero,^{120a,120b} J. Donini,³⁴ J. Dopke,¹³⁰ A. Doria,^{103a} M. T. Dova,⁷⁰ A. T. Doyle,⁵³ M. Dris,¹⁰ J. Dubbert,⁸⁸ S. Dube,¹⁵ E. Dubreuil,³⁴ E. Duchovni,¹⁷³ G. Duckeck,⁹⁹ O. A. Ducu,^{26a} D. Duda,¹⁷⁶ A. Dudarev,³⁰ F. Dudziak,⁶³ L. Dufлот,¹¹⁶ L. Duguid,⁷⁶ M. Dührssen,³⁰ M. Dunford,^{58a} H. Duran Yildiz,^{4a} M. Düren,⁵² A. Durglishvili,^{51b} M. Dwuznik,^{38a} M. Dyndal,^{38a} J. Ebke,⁹⁹ W. Edson,² N. C. Edwards,⁴⁶ W. Ehrenfeld,²¹ T. Eifert,¹⁴⁴ G. Eigen,¹⁴ K. Einsweiler,¹⁵ T. Ekelof,¹⁶⁷ M. El Kacimi,^{136c} M. Ellert,¹⁶⁷ S. Elles,⁵ F. Ellinghaus,⁸² N. Ellis,³⁰ J. Elmsheuser,⁹⁹ M. Elsing,³⁰ D. Emeliyanov,¹³⁰ Y. Enari,¹⁵⁶ O. C. Endner,⁸² M. Endo,¹¹⁷ R. Engelmann,¹⁴⁹ J. Erdmann,¹⁷⁷ A. Ereditato,¹⁷ D. Eriksson,^{147a} G. Ernis,¹⁷⁶ J. Ernst,² M. Ernst,²⁵ J. Ernwein,¹³⁷ D. Errede,¹⁶⁶ S. Errede,¹⁶⁶ E. Ertel,⁸² M. Escalier,¹¹⁶ H. Esch,⁴³ C. Escobar,¹²⁴ B. Esposito,⁴⁷ A. I. Etiennevre,¹³⁷ E. Etzion,¹⁵⁴ H. Evans,⁶⁰ A. Ezhilov,¹²² L. Fabbri,^{20a,20b} G. Facini,³¹ R. M. Fakhruddinov,¹²⁹ S. Falciano,^{133a} R. J. Falla,⁷⁷ J. Faltova,¹²⁸ Y. Fang,^{33a} M. Fanti,^{90a,90b} A. Farbin,⁸ A. Farilla,^{135a} T. Farooque,¹² S. Farrell,¹⁵ S. M. Farrington,¹⁷¹ P. Farthouat,³⁰ F. Fassi,^{136e} P. Fassnacht,³⁰ D. Fassouliotis,⁹ A. Favareto,^{50a,50b} L. Fayard,¹¹⁶ P. Federic,^{145a} O. L. Fedin,^{122,k} W. Fedorko,¹⁶⁹ M. Fehling-Kaschek,⁴⁸ S. Feigl,³⁰ L. Felgioni,⁸⁴ C. Feng,^{33d} E. J. Feng,⁶ H. Feng,⁸⁸ A. B. Fenyuk,¹²⁹ S. Fernandez Perez,³⁰ S. Ferrag,⁵³ J. Ferrando,⁵³ A. Ferrari,¹⁶⁷ P. Ferrari,¹⁰⁶ R. Ferrari,^{120a} D. E. Ferreira de Lima,⁵³ A. Ferrer,¹⁶⁸ D. Ferrere,⁴⁹ C. Ferretti,⁸⁸ A. Ferretto Parodi,^{50a,50b} M. Fiascaris,³¹ F. Fiedler,⁸² A. Filipčić,⁷⁴ M. Filipuzzi,⁴² F. Filthaut,¹⁰⁵ M. Fincke-Keeler,¹⁷⁰ K. D. Finelli,¹⁵¹ M. C. N. Fiolhais,^{125a,125c} L. Fiorini,¹⁶⁸ A. Firan,⁴⁰ A. Fischer,² J. Fischer,¹⁷⁶ W. C. Fisher,⁸⁹ E. A. Fitzgerald,²³ M. Flechl,⁴⁸ I. Fleck,¹⁴² P. Fleischmann,⁸⁸ S. Fleischmann,¹⁷⁶ G. T. Fletcher,¹⁴⁰ G. Fletcher,⁷⁵ T. Flick,¹⁷⁶ A. Floderus,⁸⁰ L. R. Flores Castillo,^{174,l} A. C. Florez Bustos,^{160b} M. J. Flowerdew,¹⁰⁰ A. Formica,¹³⁷ A. Forti,⁸³ D. Fortin,^{160a} D. Fournier,¹¹⁶ H. Fox,⁷¹ S. Fracchia,¹² P. Francavilla,⁷⁹ M. Franchini,^{20a,20b} S. Franchino,³⁰ D. Francis,³⁰ L. Franconi,¹¹⁸ M. Franklin,⁵⁷ S. Franz,⁶¹ M. Fraternali,^{120a,120b} S. T. French,²⁸ C. Friedrich,⁴² F. Friedrich,⁴⁴ D. Froidevaux,³⁰ J. A. Frost,²⁸ C. Fukunaga,¹⁵⁷ E. Fullana Torregrosa,⁸² B. G. Fulsom,¹⁴⁴ J. Fuster,¹⁶⁸ C. Gabaldon,⁵⁵ O. Gabizon,¹⁷³ A. Gabrielli,^{20a,20b} A. Gabrielli,^{133a,133b} S. Gadatsch,¹⁰⁶ S. Gadomski,⁴⁹ G. Gagliardi,^{50a,50b} P. Gagnon,⁶⁰ C. Galea,¹⁰⁵ B. Galhardo,^{125a,125c} E. J. Gallas,¹¹⁹ V. Gallo,¹⁷ B. J. Gallop,¹³⁰ P. Gallus,¹²⁷ G. Galster,³⁶ K. K. Gan,¹¹⁰ J. Gao,^{33b,h} Y. S. Gao,^{144,f} F. M. Garay Walls,⁴⁶ F. Garbersson,¹⁷⁷ C. García,¹⁶⁸ J. E. García Navarro,¹⁶⁸ M. Garcia-Sciveres,¹⁵ R. W. Gardner,³¹ N. Garelli,¹⁴⁴ V. Garonne,³⁰ C. Gatti,⁴⁷ G. Gaudio,^{120a} B. Gaur,¹⁴² L. Gauthier,⁹⁴ P. Gauzzi,^{133a,133b} I. L. Gavrilenko,⁹⁵ C. Gay,¹⁶⁹ G. Gaycken,²¹ E. N. Gazis,¹⁰ P. Ge,^{33d} Z. Gece,¹⁶⁹ C. N. P. Gee,¹³⁰ D. A. A. Geerts,¹⁰⁶ Ch. Geich-Gimbel,²¹ K. Gellerstedt,^{147a,147b} C. Gemme,^{50a} A. Gemmell,⁵³ M. H. Genest,⁵⁵ S. Gentile,^{133a,133b} M. George,⁵⁴ S. George,⁷⁶ D. Gerbaudo,¹⁶⁴ A. Gershon,¹⁵⁴ H. Ghazlane,^{136b} N. Ghodbane,³⁴ B. Giacobbe,^{20a} S. Giagu,^{133a,133b} V. Giangiobbe,¹² P. Giannetti,^{123a,123b} F. Gianotti,³⁰ B. Gibbard,²⁵ S. M. Gibson,⁷⁶ M. Gilchriese,¹⁵ T. P. S. Gillam,²⁸ D. Gillberg,³⁰ G. Gilles,³⁴ D. M. Gingrich,^{3,e} N. Giokaris,⁹ M. P. Giordani,^{165a,165c} R. Giordano,^{103a,103b} F. M. Giorgi,^{20a} F. M. Giorgi,¹⁶ P. F. Giraud,¹³⁷ D. Giugni,^{90a} C. Giuliani,⁴⁸ M. Giulini,^{58b} B. K. Gjelsten,¹¹⁸ S. Gkaitatzis,¹⁵⁵ I. Gkialas,^{155,m} L. K. Gladilin,⁹⁸ C. Glasman,⁸¹ J. Glatzer,³⁰ P. C. F. Glaysheer,⁴⁶ A. Glazov,⁴² G. L. Glonti,⁶⁴ M. Goblirsch-Kolb,¹⁰⁰ J. R. Goddard,⁷⁵ J. Godlewski,³⁰ C. Goeringer,⁸² S. Goldfarb,⁸⁸ T. Golling,¹⁷⁷ D. Golubkov,¹²⁹ A. Gomes,^{125a,125b,125d} L. S. Gomez Fajardo,⁴² R. Gonçalves,^{125a} J. Goncalves Pinto Firmino Da Costa,¹³⁷ L. Gonella,²¹ S. González de la Hoz,¹⁶⁸ G. Gonzalez Parra,¹² S. Gonzalez-Sevilla,⁴⁹ L. Goossens,³⁰ P. A. Gorbounov,⁹⁶ H. A. Gordon,²⁵ I. Gorelov,¹⁰⁴ B. Gorini,³⁰ E. Gorini,^{72a,72b} A. Gorišek,⁷⁴ E. Gornicki,³⁹ A. T. Goshaw,⁶ C. Gössling,⁴³ M. I. Gostkin,⁶⁴ M. Gouighri,^{136a} D. Goujdami,^{136c} M. P. Goulette,⁴⁹ A. G. Goussiou,¹³⁹ C. Goy,⁵ S. Gozpinar,²³ H. M. X. Grabas,¹³⁷ L. Graber,⁵⁴ I. Grabowska-Bold,^{38a} P. Grafström,^{20a,20b} K.-J. Grahm,⁴² J. Gramling,⁴⁹ E. Gramstad,¹¹⁸ S. Grancagnolo,¹⁶ V. Grassi,¹⁴⁹ V. Gratchev,¹²² H. M. Gray,³⁰ E. Graziani,^{135a} O. G. Grebenyuk,¹²² Z. D. Greenwood,^{78,n} K. Gregersen,⁷⁷ I. M. Gregor,⁴² P. Grenier,¹⁴⁴ J. Griffiths,⁸ A. A. Grillo,¹³⁸ K. Grimm,⁷¹ S. Grinstein,^{12,o} Ph. Gris,³⁴ Y. V. Grishkevich,⁹⁸ J.-F. Grivaz,¹¹⁶ J. P. Grohs,⁴⁴ A. Grohsjean,⁴² E. Gross,¹⁷³ J. Grosse-Knetter,⁵⁴ G. C. Grossi,^{134a,134b} J. Groth-Jensen,¹⁷³ Z. J. Grout,¹⁵⁰ L. Guan,^{33b} F. Guescini,⁴⁹ D. Guest,¹⁷⁷ O. Gueta,¹⁵⁴ C. Guicheney,³⁴ E. Guido,^{50a,50b} T. Guillemin,¹¹⁶ S. Guindon,² U. Gul,⁵³ C. Gumpert,⁴⁴ J. Gunther,¹²⁷ J. Guo,³⁵ S. Gupta,¹¹⁹ P. Gutierrez,¹¹² N. G. Gutierrez Ortiz,⁵³ C. Gutsche,⁷⁷ N. Guttman,¹⁵⁴ C. Guyot,¹³⁷ C. Gwenlan,¹¹⁹ C. B. Gwilliam,⁷³ A. Haas,¹⁰⁹ C. Haber,¹⁵ H. K. Hadavand,⁸ N. Haddad,^{136e} P. Haefner,²¹ S. Hageböck,²¹ Z. Hajduk,³⁹ H. Hakobyan,¹⁷⁸ M. Haleem,⁴² D. Hall,¹¹⁹ G. Halladjian,⁸⁹ K. Hamacher,¹⁷⁶ P. Hamal,¹¹⁴ K. Hamano,¹⁷⁰ M. Hamer,⁵⁴ A. Hamilton,^{146a} S. Hamilton,¹⁶² G. N. Hamity,^{146c} P. G. Hamnett,⁴² L. Han,^{33b} K. Hanagaki,¹¹⁷ K. Hanawa,¹⁵⁶ M. Hance,¹⁵ P. Hanke,^{58a} R. Hanna,¹³⁷ J. B. Hansen,³⁶ J. D. Hansen,³⁶ P. H. Hansen,³⁶ K. Hara,¹⁶¹ A. S. Hard,¹⁷⁴ T. Harenberg,¹⁷⁶

F. Hariri,¹¹⁶ S. Harkusha,⁹¹ D. Harper,⁸⁸ R. D. Harrington,⁴⁶ O. M. Harris,¹³⁹ P. F. Harrison,¹⁷¹ F. Hartjes,¹⁰⁶ M. Hasegawa,⁶⁶ S. Hasegawa,¹⁰² Y. Hasegawa,¹⁴¹ A. Hasib,¹¹² S. Hassani,¹³⁷ S. Haug,¹⁷ M. Hauschild,³⁰ R. Hauser,⁸⁹ M. Havranek,¹²⁶ C. M. Hawkes,¹⁸ R. J. Hawkings,³⁰ A. D. Hawkins,⁸⁰ T. Hayashi,¹⁶¹ D. Hayden,⁸⁹ C. P. Hays,¹¹⁹ H. S. Hayward,⁷³ S. J. Haywood,¹³⁰ S. J. Head,¹⁸ T. Heck,⁸² V. Hedberg,⁸⁰ L. Heelan,⁸ S. Heim,¹²¹ T. Heim,¹⁷⁶ B. Heinemann,¹⁵ L. Heinrich,¹⁰⁹ J. Hejbal,¹²⁶ L. Helary,²² C. Heller,⁹⁹ M. Heller,³⁰ S. Hellman,^{147a,147b} D. Hellmich,²¹ C. Helsens,³⁰ J. Henderson,¹¹⁹ R. C. W. Henderson,⁷¹ Y. Heng,¹⁷⁴ C. Hengler,⁴² A. Henrichs,¹⁷⁷ A. M. Henriques Correia,³⁰ S. Henrot-Versille,¹¹⁶ C. Hensel,⁵⁴ G. H. Herbert,¹⁶ Y. Hernández Jiménez,¹⁶⁸ R. Herrberg-Schubert,¹⁶ G. Herten,⁴⁸ R. Hertenberger,⁹⁹ L. Hervas,³⁰ G. G. Hesketh,⁷⁷ N. P. Hessey,¹⁰⁶ R. Hickling,⁷⁵ E. Higón-Rodríguez,¹⁶⁸ E. Hill,¹⁷⁰ J. C. Hill,²⁸ K. H. Hiller,⁴² S. Hillert,²¹ S. J. Hillier,¹⁸ I. Hinchliffe,¹⁵ E. Hines,¹²¹ M. Hirose,¹⁵⁸ D. Hirschbuehl,¹⁷⁶ J. Hobbs,¹⁴⁹ N. Hod,¹⁰⁶ M. C. Hodgkinson,¹⁴⁰ P. Hodgson,¹⁴⁰ A. Hoecker,³⁰ M. R. Hoferkamp,¹⁰⁴ F. Hoenig,⁹⁹ J. Hoffman,⁴⁰ D. Hoffmann,⁸⁴ J. I. Hofmann,^{58a} M. Hohlfield,⁸² T. R. Holmes,¹⁵ T. M. Hong,¹²¹ L. Hooft van Huysduynen,¹⁰⁹ W. H. Hopkins,¹¹⁵ Y. Horii,¹⁰² J.-Y. Hostachy,⁵⁵ S. Hou,¹⁵² A. Houmada,^{136a} J. Howard,¹¹⁹ J. Howarth,⁴² M. Hrabovsky,¹¹⁴ I. Hristova,¹⁶ J. Hrivnac,¹¹⁶ T. Hryn'ova,⁵ C. Hsu,^{146c} P. J. Hsu,⁸² S.-C. Hsu,¹³⁹ D. Hu,³⁵ X. Hu,²⁵ Y. Huang,⁴² Z. Hubacek,³⁰ F. Hubaut,⁸⁴ F. Huegging,²¹ T. B. Huffman,¹¹⁹ E. W. Hughes,³⁵ G. Hughes,⁷¹ M. Huhtinen,³⁰ T. A. Hülsing,⁸² M. Hurwitz,¹⁵ N. Huseynov,^{64,c} J. Huston,⁸⁹ J. Huth,⁵⁷ G. Iacobucci,⁴⁹ G. Iakovidis,¹⁰ I. Ibragimov,¹⁴² L. Iconomidou-Fayard,¹¹⁶ E. Ideal,¹⁷⁷ P. Iengo,^{103a} O. Igonkina,¹⁰⁶ T. Iizawa,¹⁷² Y. Ikegami,⁶⁵ K. Ikematsu,¹⁴² M. Ikeno,⁶⁵ Y. Ilchenko,^{31,p} D. Iliadis,¹⁵⁵ N. Ilic,¹⁵⁹ Y. Inamaru,⁶⁶ T. Ince,¹⁰⁰ P. Ioannou,⁹ M. Iodice,^{135a} K. Iordanidou,⁹ V. Ippolito,⁵⁷ A. Irls Quiles,¹⁶⁸ C. Isaksson,¹⁶⁷ M. Ishino,⁶⁷ M. Ishitsuka,¹⁵⁸ R. Ishmukhametov,¹¹⁰ C. Issever,¹¹⁹ S. Istin,^{19a} J. M. Iturbe Ponce,⁸³ R. Iuppa,^{134a,134b} J. Ivarsson,⁸⁰ W. Iwanski,³⁹ H. Iwasaki,⁶⁵ J. M. Izen,⁴¹ V. Izzo,^{103a} B. Jackson,¹²¹ M. Jackson,⁷³ P. Jackson,¹ M. R. Jaekel,³⁰ V. Jain,² K. Jakobs,⁴⁸ S. Jakobsen,³⁰ T. Jakoubek,¹²⁶ J. Jakubek,¹²⁷ D. O. Jamin,¹⁵² D. K. Jana,⁷⁸ E. Jansen,⁷⁷ H. Jansen,³⁰ J. Janssen,²¹ M. Janus,¹⁷¹ G. Jarlskog,⁸⁰ N. Javadov,^{64,c} T. Javůrek,⁴⁸ L. Jeanty,¹⁵ J. Jejelava,^{51a,q} G.-Y. Jeng,¹⁵¹ D. Jennens,⁸⁷ P. Jenni,^{48,r} J. Jentzsch,⁴³ C. Jeske,¹⁷¹ S. Jézéquel,⁵ H. Ji,¹⁷⁴ J. Jia,¹⁴⁹ Y. Jiang,^{33b} M. Jimenez Belenguer,⁴² S. Jin,^{33a} A. Jinaru,^{26a} O. Jinnouchi,¹⁵⁸ M. D. Joergensen,³⁶ K. E. Johansson,^{147a,147b} P. Johansson,¹⁴⁰ K. A. Johns,⁷ K. Jon-And,^{147a,147b} G. Jones,¹⁷¹ R. W. L. Jones,⁷¹ T. J. Jones,⁷³ J. Jongmanns,^{58a} P. M. Jorge,^{125a,125b} K. D. Joshi,⁸³ J. Jovicevic,¹⁴⁸ X. Ju,¹⁷⁴ C. A. Jung,⁴³ R. M. Jungst,³⁰ P. Jussel,⁶¹ A. Juste Rozas,^{12,o} M. Kaci,¹⁶⁸ A. Kaczmarska,³⁹ M. Kado,¹¹⁶ H. Kagan,¹¹⁰ M. Kagan,¹⁴⁴ E. Kajomovitz,⁴⁵ C. W. Kalderon,¹¹⁹ S. Kama,⁴⁰ A. Kamenshchikov,¹²⁹ N. Kanaya,¹⁵⁶ M. Kaneda,³⁰ S. Kaneti,²⁸ V. A. Kantserov,⁹⁷ J. Kanzaki,⁶⁵ B. Kaplan,¹⁰⁹ A. Kapliy,³¹ D. Kar,⁵³ K. Karakostas,¹⁰ N. Karastathis,¹⁰ M. J. Kareem,⁵⁴ M. Karnevskiy,⁸² S. N. Karpov,⁶⁴ Z. M. Karpova,⁶⁴ K. Karthik,¹⁰⁹ V. Kartvelishvili,⁷¹ A. N. Karyukhin,¹²⁹ L. Kashif,¹⁷⁴ G. Kasieczka,^{58b} R. D. Kass,¹¹⁰ A. Kastanas,¹⁴ Y. Kataoka,¹⁵⁶ A. Katre,⁴⁹ J. Katzy,⁴² V. Kaushik,⁷ K. Kawagoe,⁶⁹ T. Kawamoto,¹⁵⁶ G. Kawamura,⁵⁴ S. Kazama,¹⁵⁶ V. F. Kazanin,¹⁰⁸ M. Y. Kazarinov,⁶⁴ R. Keeler,¹⁷⁰ R. Kehoe,⁴⁰ M. Keil,⁵⁴ J. S. Keller,⁴² J. J. Kempster,⁷⁶ H. Keoshkerian,⁵ O. Kepka,¹²⁶ B. P. Kerševan,⁷⁴ S. Kersten,¹⁷⁶ K. Kessoku,¹⁵⁶ J. Keung,¹⁵⁹ F. Khalil-zada,¹¹ H. Khandanyan,^{147a,147b} A. Khanov,¹¹³ A. Khodinov,⁹⁷ A. Khomich,^{58a} T. J. Khoo,²⁸ G. Khorauli,²¹ A. Khoroshilov,¹⁷⁶ V. Khovanskiy,⁹⁶ E. Khramov,⁶⁴ J. Khubua,^{51b} H. Y. Kim,⁸ H. Kim,^{147a,147b} S. H. Kim,¹⁶¹ N. Kimura,¹⁷² O. Kind,¹⁶ B. T. King,⁷³ M. King,¹⁶⁸ R. S. B. King,¹¹⁹ S. B. King,¹⁶⁹ J. Kirk,¹³⁰ A. E. Kiryunin,¹⁰⁰ T. Kishimoto,⁶⁶ D. Kisieleska,^{38a} F. Kiss,⁴⁸ T. Kittelmann,¹²⁴ K. Kiuchi,¹⁶¹ E. Kladiva,^{145b} M. Klein,⁷³ U. Klein,⁷³ K. Kleinknecht,⁸² P. Klimek,^{147a,147b} A. Klimentov,²⁵ R. Klingenberg,⁴³ J. A. Klinger,⁸³ T. Klioutchnikova,³⁰ P. F. Klok,¹⁰⁵ E.-E. Kluge,^{58a} P. Kluit,¹⁰⁶ S. Kluth,¹⁰⁰ E. Kneringer,⁶¹ E. B. F. G. Knoop,⁸⁴ A. Knue,⁵³ D. Kobayashi,¹⁵⁸ T. Kobayashi,¹⁵⁶ M. Kobel,⁴⁴ M. Kocian,¹⁴⁴ P. Kodys,¹²⁸ P. Koevesarki,²¹ T. Koffas,²⁹ E. Koffeman,¹⁰⁶ L. A. Kogan,¹¹⁹ S. Kohlmann,¹⁷⁶ Z. Kohout,¹²⁷ T. Kohriki,⁶⁵ T. Koi,¹⁴⁴ H. Kolanoski,¹⁶ I. Koletsou,⁵ J. Koll,⁸⁹ A. A. Komar,^{95,a} Y. Komori,¹⁵⁶ T. Kondo,⁶⁵ N. Kondrashova,⁴² K. Köneke,⁴⁸ A. C. König,¹⁰⁵ S. König,⁸² T. Kono,^{65,s} R. Konoplich,^{109,t} N. Konstantinidis,⁷⁷ R. Kopeliansky,¹⁵³ S. Koperny,^{38a} L. Köpke,⁸² A. K. Kopp,⁴⁸ K. Korcyl,³⁹ K. Kordas,¹⁵⁵ A. Korn,⁷⁷ A. A. Korol,^{108,u} I. Korolkov,¹² E. V. Korolkova,¹⁴⁰ V. A. Korotkov,¹²⁹ O. Kortner,¹⁰⁰ S. Kortner,¹⁰⁰ V. V. Kostyukhin,²¹ V. M. Kotov,⁶⁴ A. Kotwal,⁴⁵ C. Kourkoumelis,⁹ V. Kouskoura,¹⁵⁵ A. Koutsman,^{160a} R. Kowalewski,¹⁷⁰ T. Z. Kowalski,^{38a} W. Kozanecki,¹³⁷ A. S. Kozhin,¹²⁹ V. Kral,¹²⁷ V. A. Kramarenko,⁹⁸ G. Kramberger,⁷⁴ D. Krasnoperov,⁹⁷ M. W. Krasny,⁷⁹ A. Krasznahorkay,³⁰ J. K. Kraus,²¹ A. Kravchenko,²⁵ S. Kreiss,¹⁰⁹ M. Kretz,^{58c} J. Kretzschmar,⁷³ K. Kreuzfeldt,⁵² P. Krieger,¹⁵⁹ K. Kroeninger,⁵⁴ H. Kroha,¹⁰⁰ J. Kroll,¹²¹ J. Kroseberg,²¹ J. Krstic,^{13a} U. Kruchonak,⁶⁴ H. Krüger,²¹ T. Kruker,¹⁷ N. Krumnack,⁶³ Z. V. Krumshteyn,⁶⁴ A. Kruse,¹⁷⁴ M. C. Kruse,⁴⁵ M. Kruskal,²² T. Kubota,⁸⁷ S. Kuday,^{4a} S. Kuehn,⁴⁸ A. Kugel,^{58c} A. Kuhl,¹³⁸ T. Kuhl,⁴² V. Kukhtin,⁶⁴ Y. Kulchitsky,⁹¹ S. Kuleshov,^{32b} M. Kuna,^{133a,133b} J. Kunkle,¹²¹ A. Kupco,¹²⁶ H. Kurashige,⁶⁶ Y. A. Kurochkin,⁹¹ R. Kurumida,⁶⁶ V. Kus,¹²⁶ E. S. Kuwertz,¹⁴⁸

M. Kuze,¹⁵⁸ J. Kvita,¹¹⁴ A. La Rosa,⁴⁹ L. La Rotonda,^{37a,37b} C. Lacasta,¹⁶⁸ F. Lacava,^{133a,133b} J. Lacey,²⁹ H. Lacker,¹⁶ D. Lacour,⁷⁹ V. R. Lacuesta,¹⁶⁸ E. Ladygin,⁶⁴ R. Lafaye,⁵ B. Laforge,⁷⁹ T. Lagouri,¹⁷⁷ S. Lai,⁴⁸ H. Laier,^{58a} L. Lambourne,⁷⁷ S. Lammers,⁶⁰ C. L. Lampen,⁷ W. Lampl,⁷ E. Lançon,¹³⁷ U. Landgraf,⁴⁸ M. P. J. Landon,⁷⁵ V. S. Lang,^{58a} A. J. Lankford,¹⁶⁴ F. Lanni,²⁵ K. Lantzsck,³⁰ S. Laplace,⁷⁹ C. Lapoire,²¹ J. F. Laporte,¹³⁷ T. Lari,^{90a} F. Lasagni Manghi,^{20a,20b} M. Lassnig,³⁰ P. Laurelli,⁴⁷ W. Lavrijsen,¹⁵ A. T. Law,¹³⁸ P. Laycock,⁷³ O. Le Dortz,⁷⁹ E. Le Guirriec,⁸⁴ E. Le Menedeu,¹² T. LeCompte,⁶ F. Ledroit-Guillon,⁵⁵ C. A. Lee,¹⁵² H. Lee,¹⁰⁶ J. S. H. Lee,¹¹⁷ S. C. Lee,¹⁵² L. Lee,¹ G. Lefebvre,⁷⁹ M. Lefebvre,¹⁷⁰ F. Legger,⁹⁹ C. Leggett,¹⁵ A. Lehan,⁷³ M. Lehmacher,²¹ G. Lehmann Miotto,³⁰ X. Lei,⁷ W. A. Leight,²⁹ A. Leisos,¹⁵⁵ A. G. Leister,¹⁷⁷ M. A. L. Leite,^{24d} R. Leitner,¹²⁸ D. Lellouch,¹⁷³ B. Lemmer,⁵⁴ K. J. C. Leney,⁷⁷ T. Lenz,²¹ G. Lenzen,¹⁷⁶ B. Lenzi,³⁰ R. Leone,⁷ S. Leone,^{123a,123b} C. Leonidopoulos,⁴⁶ S. Leontsinis,¹⁰ C. Leroy,⁹⁴ C. G. Lester,²⁸ C. M. Lester,¹²¹ M. Levchenko,¹²² J. Levêque,⁵ D. Levin,⁸⁸ L. J. Levinson,¹⁷³ M. Levy,¹⁸ A. Lewis,¹¹⁹ G. H. Lewis,¹⁰⁹ A. M. Leyko,²¹ M. Leyton,⁴¹ B. Li,^{33b,v} B. Li,⁸⁴ H. Li,¹⁴⁹ H. L. Li,³¹ L. Li,⁴⁵ L. Li,^{33e} S. Li,⁴⁵ Y. Li,^{33c,w} Z. Liang,¹³⁸ H. Liao,³⁴ B. Liberti,^{134a} P. Lichard,³⁰ K. Lie,¹⁶⁶ J. Liebal,²¹ W. Liebig,¹⁴ C. Limbach,²¹ A. Limosani,⁸⁷ S. C. Lin,^{152,x} T. H. Lin,⁸² F. Linde,¹⁰⁶ B. E. Lindquist,¹⁴⁹ J. T. Linnemann,⁸⁹ E. Lipeles,¹²¹ A. Lipniacka,¹⁴ M. Lisovyi,⁴² T. M. Liss,¹⁶⁶ D. Lissauer,²⁵ A. Lister,¹⁶⁹ A. M. Litke,¹³⁸ B. Liu,¹⁵² D. Liu,¹⁵² J. B. Liu,^{33b} K. Liu,^{33b,y} L. Liu,⁸⁸ M. Liu,⁴⁵ M. Liu,^{33b} Y. Liu,^{33b} M. Livan,^{120a,120b} S. S. A. Livermore,¹¹⁹ A. Lleres,⁵⁵ J. Llorente Merino,⁸¹ S. L. Lloyd,⁷⁵ F. Lo Sterzo,¹⁵² E. Lobodzinska,⁴² P. Loch,⁷ W. S. Lockman,¹³⁸ T. Loddenkoetter,²¹ F. K. Loebinger,⁸³ A. E. Loevschall-Jensen,³⁶ A. Loginov,¹⁷⁷ T. Lohse,¹⁶ K. Lohwasser,⁴² M. Lokajicek,¹²⁶ V. P. Lombardo,⁵ B. A. Long,²² J. D. Long,⁸⁸ R. E. Long,⁷¹ L. Lopes,^{125a} D. Lopez Mateos,⁵⁷ B. Lopez Paredes,¹⁴⁰ I. Lopez Paz,¹² J. Lorenz,⁹⁹ N. Lorenzo Martinez,⁶⁰ M. Losada,¹⁶³ P. Loscutoff,¹⁵ X. Lou,⁴¹ A. Lounis,¹¹⁶ J. Love,⁶ P. A. Love,⁷¹ A. J. Lowe,^{144,f} F. Lu,^{33a} N. Lu,⁸⁸ H. J. Lubatti,¹³⁹ C. Luci,^{133a,133b} A. Lucotte,⁵⁵ F. Luehring,⁶⁰ W. Lukas,⁶¹ L. Luminari,^{133a} O. Lundberg,^{147a,147b} B. Lund-Jensen,¹⁴⁸ M. Lungwitz,⁸² D. Lynn,²⁵ R. Lysak,¹²⁶ E. Lytken,⁸⁰ H. Ma,²⁵ L. L. Ma,^{33d} G. Maccarrone,⁴⁷ A. Macchiolo,¹⁰⁰ J. Machado Miguens,^{125a,125b} D. Macina,³⁰ D. Madaffari,⁸⁴ R. Madar,⁴⁸ H. J. Maddocks,⁷¹ W. F. Mader,⁴⁴ A. Madsen,¹⁶⁷ M. Maeno,⁸ T. Maeno,²⁵ E. Magradze,⁵⁴ K. Mahboubi,⁴⁸ J. Mahlstedt,¹⁰⁶ S. Mahmoud,⁷³ C. Maiani,¹³⁷ C. Maidantchik,^{24a} A. A. Maier,¹⁰⁰ A. Maio,^{125a,125b,125d} S. Majewski,¹¹⁵ Y. Makida,⁶⁵ N. Makovec,¹¹⁶ P. Mal,^{137,z} B. Malaescu,⁷⁹ Pa. Malecki,³⁹ V. P. Maleev,¹²² F. Malek,⁵⁵ U. Mallik,⁶² D. Malon,⁶ C. Malone,¹⁴⁴ S. Maltezos,¹⁰ V. M. Malyshev,¹⁰⁸ S. Malyukov,³⁰ J. Mamuzic,^{13b} B. Mandelli,³⁰ L. Mandelli,^{90a} I. Mandić,⁷⁴ R. Mandrysch,⁶² J. Maneira,^{125a,125b} A. Manfredini,¹⁰⁰ L. Manhaes de Andrade Filho,^{24b} J. A. Manjarres Ramos,^{160b} A. Mann,⁹⁹ P. M. Manning,¹³⁸ A. Manousakis-Katsikakis,⁹ B. Mansoulie,¹³⁷ R. Mantifel,⁸⁶ L. Mapelli,³⁰ L. March,¹⁶⁸ J. F. Marchand,²⁹ G. Marchiori,⁷⁹ M. Marcisovsky,¹²⁶ C. P. Marino,¹⁷⁰ M. Marjanovic,^{13a} C. N. Marques,^{125a} F. Marroquim,^{24a} S. P. Marsden,⁸³ Z. Marshall,¹⁵ L. F. Marti,¹⁷ S. Marti-Garcia,¹⁶⁸ B. Martin,³⁰ B. Martin,⁸⁹ T. A. Martin,¹⁷¹ V. J. Martin,⁴⁶ B. Martin dit Latour,¹⁴ H. Martinez,¹³⁷ M. Martinez,^{12,o} S. Martin-Haugh,¹³⁰ A. C. Martyniuk,⁷⁷ M. Marx,¹³⁹ F. Marzano,^{133a} A. Marzin,³⁰ L. Masetti,⁸² T. Mashimo,¹⁵⁶ R. Mashinistov,⁹⁵ J. Masik,⁸³ A. L. Maslennikov,¹⁰⁸ I. Massa,^{20a,20b} L. Massa,^{20a,20b} N. Massol,⁵ P. Mastrandrea,¹⁴⁹ A. Mastroberardino,^{37a,37b} T. Masubuchi,¹⁵⁶ P. Mättig,¹⁷⁶ J. Mattmann,⁸² J. Maurer,^{26a} S. J. Maxfield,⁷³ D. A. Maximov,^{108,u} R. Mazini,¹⁵² L. Mazzaferro,^{134a,134b} G. Mc Goldrick,¹⁵⁹ S. P. Mc Kee,⁸⁸ A. McCann,⁸⁸ R. L. McCarthy,¹⁴⁹ T. G. McCarthy,²⁹ N. A. McCubbin,¹³⁰ K. W. McFarlane,^{56,a} J. A. McFayden,⁷⁷ G. Mchedlidze,⁵⁴ S. J. McMahon,¹³⁰ R. A. McPherson,^{170,j} J. Mechnich,¹⁰⁶ M. Medinnis,⁴² S. Meehan,³¹ S. Mehlhase,⁹⁹ A. Mehta,⁷³ K. Meier,^{58a} C. Meineck,⁹⁹ B. Meirose,⁸⁰ C. Melachrinou,³¹ B. R. Mellado Garcia,^{146c} F. Meloni,¹⁷ A. Mengarelli,^{20a,20b} S. Menke,¹⁰⁰ E. Meoni,¹⁶² K. M. Mercurio,⁵⁷ S. Mergelmeyer,²¹ N. Meric,¹³⁷ P. Mermod,⁴⁹ L. Merola,^{103a,103b} C. Meroni,^{90a} F. S. Merritt,³¹ H. Merritt,¹¹⁰ A. Messina,^{30,aa} J. Metcalfe,²⁵ A. S. Mete,¹⁶⁴ C. Meyer,⁸² C. Meyer,¹²¹ J-P. Meyer,¹³⁷ J. Meyer,³⁰ R. P. Middleton,¹³⁰ S. Migas,⁷³ L. Mijović,²¹ G. Mikenberg,¹⁷³ M. Mikestikova,¹²⁶ M. Mikuž,⁷⁴ A. Milic,³⁰ D. W. Miller,³¹ C. Mills,⁴⁶ A. Milov,¹⁷³ D. A. Milstead,^{147a,147b} D. Milstein,¹⁷³ A. A. Minaenko,¹²⁹ I. A. Minashvili,⁶⁴ A. I. Mincer,¹⁰⁹ B. Mindur,^{38a} M. Mineev,⁶⁴ Y. Ming,¹⁷⁴ L. M. Mir,¹² G. Mirabelli,^{133a} T. Mitani,¹⁷² J. Mitrevski,⁹⁹ V. A. Mitsou,¹⁶⁸ S. Mitsui,⁶⁵ A. Miucci,⁴⁹ P. S. Miyagawa,¹⁴⁰ J. U. Mjörnmark,⁸⁰ T. Moe,^{147a,147b} K. Mochizuki,⁸⁴ S. Mohapatra,³⁵ W. Mohr,⁴⁸ S. Molander,^{147a,147b} R. Moles-Valls,¹⁶⁸ K. Mönig,⁴² C. Monini,⁵⁵ J. Monk,³⁶ E. Monnier,⁸⁴ J. Montejo Berlingen,¹² F. Monticelli,⁷⁰ S. Monzani,^{133a,133b} R. W. Moore,³ N. Morange,⁶² D. Moreno,⁸² M. Moreno Llácer,⁵⁴ P. Morettini,^{50a} M. Morgenstern,⁴⁴ M. Morii,⁵⁷ S. Moritz,⁸² A. K. Morley,¹⁴⁸ G. Mornacchi,³⁰ J. D. Morris,⁷⁵ L. Morvaj,¹⁰² H. G. Moser,¹⁰⁰ M. Mosidze,^{51b} J. Moss,¹¹⁰ K. Motohashi,¹⁵⁸ R. Mount,¹⁴⁴ E. Mountricha,²⁵ S. V. Mouraviev,^{95,a} E. J. W. Moyses,⁸⁵ S. Muanza,⁸⁴ R. D. Mudd,¹⁸ F. Mueller,^{58a} J. Mueller,¹²⁴ K. Mueller,²¹ T. Mueller,²⁸ T. Mueller,⁸² D. Muenstermann,⁴⁹ Y. Munwes,¹⁵⁴ J. A. Murillo Quijada,¹⁸ W. J. Murray,^{171,130} H. Musheghyan,⁵⁴

E. Musto,¹⁵³ A. G. Myagkov,^{129,bb} M. Myska,¹²⁷ O. Nackenhorst,⁵⁴ J. Nadal,⁵⁴ K. Nagai,⁶¹ R. Nagai,¹⁵⁸ Y. Nagai,⁸⁴ K. Nagano,⁶⁵ A. Nagarkar,¹¹⁰ Y. Nagasaka,⁵⁹ M. Nagel,¹⁰⁰ A. M. Nairz,³⁰ Y. Nakahama,³⁰ K. Nakamura,⁶⁵ T. Nakamura,¹⁵⁶ I. Nakano,¹¹¹ H. Namasivayam,⁴¹ G. Nanava,²¹ R. Narayan,^{58b} T. Nattermann,²¹ T. Naumann,⁴² G. Navarro,¹⁶³ R. Nayyar,⁷ H. A. Neal,⁸⁸ P. Yu. Nechaeva,⁹⁵ T. J. Neep,⁸³ P. D. Nef,¹⁴⁴ A. Negri,^{120a,120b} G. Negri,³⁰ M. Negrini,^{20a} S. Nektarijevic,⁴⁹ A. Nelson,¹⁶⁴ T. K. Nelson,¹⁴⁴ S. Nemecek,¹²⁶ P. Nemethy,¹⁰⁹ A. A. Nepomuceno,^{24a} M. Nessi,^{30,cc} M. S. Neubauer,¹⁶⁶ M. Neumann,¹⁷⁶ R. M. Neves,¹⁰⁹ P. Nevski,²⁵ P. R. Newman,¹⁸ D. H. Nguyen,⁶ R. B. Nickerson,¹¹⁹ R. Nicolaidou,¹³⁷ B. Nicquevert,³⁰ J. Nielsen,¹³⁸ N. Nikiforou,³⁵ A. Nikiforov,¹⁶ V. Nikolaenko,^{129,bb} I. Nikolic-Audit,⁷⁹ K. Nikolics,⁴⁹ K. Nikolopoulos,¹⁸ P. Nilsson,⁸ Y. Ninomiya,¹⁵⁶ A. Nisati,^{133a} R. Nisius,¹⁰⁰ T. Nobe,¹⁵⁸ L. Nodulman,⁶ M. Nomachi,¹¹⁷ I. Nomidis,²⁹ S. Norberg,¹¹² M. Nordberg,³⁰ O. Novgorodova,⁴⁴ S. Nowak,¹⁰⁰ M. Nozaki,⁶⁵ L. Nozka,¹¹⁴ K. Ntekas,¹⁰ G. Nunes Hanninger,⁸⁷ T. Nunnemann,⁹⁹ E. Nurse,⁷⁷ F. Nuti,⁸⁷ B. J. O'Brien,⁴⁶ F. O'Grady,⁷ D. C. O'Neil,¹⁴³ V. O'Shea,⁵³ F. G. Oakham,^{29,e} H. Oberlack,¹⁰⁰ T. Obermann,²¹ J. Ocariz,⁷⁹ A. Ochi,⁶⁶ M. I. Ochoa,⁷⁷ S. Oda,⁶⁹ S. Odaka,⁶⁵ H. Ogren,⁶⁰ A. Oh,⁸³ S. H. Oh,⁴⁵ C. C. Ohm,¹⁵ H. Ohman,¹⁶⁷ W. Okamura,¹¹⁷ H. Okawa,²⁵ Y. Okumura,³¹ T. Okuyama,¹⁵⁶ A. Olariu,^{26a} A. G. Olchevski,⁶⁴ S. A. Olivares Pino,⁴⁶ D. Oliveira Damazio,²⁵ E. Oliver Garcia,¹⁶⁸ A. Olszewski,³⁹ J. Olszowska,³⁹ A. Onofre,^{125a,125e} P. U. E. Onyisi,^{31,p} C. J. Oram,^{160a} M. J. Oreglia,³¹ Y. Oren,¹⁵⁴ D. Orestano,^{135a,135b} N. Orlando,^{72a,72b} C. Oropeza Barrera,⁵³ R. S. Orr,¹⁵⁹ B. Osculati,^{50a,50b} R. Ospanov,¹²¹ G. Otero y Garzon,²⁷ H. Otono,⁶⁹ M. Ouchrif,^{136d} E. A. Ouellette,¹⁷⁰ F. Ould-Saada,¹¹⁸ A. Ouraou,¹³⁷ K. P. Oussoren,¹⁰⁶ Q. Ouyang,^{33a} A. Ovcharova,¹⁵ M. Owen,⁸³ V. E. Ozcan,^{19a} N. Ozturk,⁸ K. Pachal,¹¹⁹ A. Pacheco Pages,¹² C. Padilla Aranda,¹² M. Pagáčová,⁴⁸ S. Pagan Griso,¹⁵ E. Paganis,¹⁴⁰ C. Pahl,¹⁰⁰ F. Paige,²⁵ P. Pais,⁸⁵ K. Pajchel,¹¹⁸ G. Palacino,^{160b} S. Palestini,³⁰ M. Palka,^{38b} D. Pallin,³⁴ A. Palma,^{125a,125b} J. D. Palmer,¹⁸ Y. B. Pan,¹⁷⁴ E. Panagiotopoulou,¹⁰ J. G. Panduro Vazquez,⁷⁶ P. Pani,¹⁰⁶ N. Panikashvili,⁸⁸ S. Panitkin,²⁵ D. Pantea,^{26a} L. Paolozzi,^{134a,134b} Th. D. Papadopoulou,¹⁰ K. Papageorgiou,^{155,m} A. Paramonov,⁶ D. Paredes Hernandez,³⁴ M. A. Parker,²⁸ F. Parodi,^{50a,50b} J. A. Parsons,³⁵ U. Parzefall,⁴⁸ E. Pasqualucci,^{133a} S. Passaggio,^{50a} A. Passeri,^{135a} F. Pastore,^{135a,135b,a} Fr. Pastore,⁷⁶ G. Pásztor,²⁹ S. Patariaia,¹⁷⁶ N. D. Patel,¹⁵¹ J. R. Pater,⁸³ S. Patricelli,^{103a,103b} T. Pauly,³⁰ J. Pearce,¹⁷⁰ L. E. Pedersen,³⁶ M. Pedersen,¹¹⁸ S. Pedraza Lopez,¹⁶⁸ R. Pedro,^{125a,125b} S. V. Peleganchuk,¹⁰⁸ D. Pelikan,¹⁶⁷ H. Peng,^{33b} B. Penning,³¹ J. Penwell,⁶⁰ D. V. Perepelitsa,²⁵ E. Perez Codina,^{160a} M. T. Pérez García-Estañ,¹⁶⁸ V. Perez Reale,³⁵ L. Perini,^{90a,90b} H. Pernegger,³⁰ S. Perrella,^{103a,103b} R. Perrino,^{72a} R. Peschke,⁴² V. D. Peshekhonov,⁶⁴ K. Peters,³⁰ R. F. Y. Peters,⁸³ B. A. Petersen,³⁰ T. C. Petersen,³⁶ E. Petit,⁴² A. Petridis,^{147a,147b} C. Petridou,¹⁵⁵ E. Petrolu,^{133a} F. Petrucci,^{135a,135b} N. E. Pettersson,¹⁵⁸ R. Pezoa,^{32b} P. W. Phillips,¹³⁰ G. Piacquadio,¹⁴⁴ E. Pianori,¹⁷¹ A. Picazio,⁴⁹ E. Piccaro,⁷⁵ M. Piccinini,^{20a,20b} R. Piegai,²⁷ D. T. Pignotti,¹¹⁰ J. E. Pilcher,³¹ A. D. Pilkington,⁷⁷ J. Pina,^{125a,125b,125d} M. Pinamonti,^{165a,165c,dd} A. Pinder,¹¹⁹ J. L. Pinfold,³ A. Pingel,³⁶ B. Pinto,^{125a} S. Pires,⁷⁹ M. Pitt,¹⁷³ C. Pizio,^{90a,90b} L. Plazak,^{145a} M.-A. Pleier,²⁵ V. Pleskot,¹²⁸ E. Plotnikova,⁶⁴ P. Plucinski,^{147a,147b} S. Poddar,^{58a} F. Podlyski,³⁴ R. Poettgen,⁸² L. Poggioli,¹¹⁶ D. Pohl,²¹ M. Pohl,⁴⁹ G. Polesello,^{120a} A. Policicchio,^{37a,37b} R. Polifka,¹⁵⁹ A. Polini,^{20a} C. S. Pollard,⁴⁵ V. Polychronakos,²⁵ K. Pommès,³⁰ L. Pontecorvo,^{133a} B. G. Pope,⁸⁹ G. A. Popeneciu,^{26b} D. S. Popovic,^{13a} A. Poppleton,³⁰ X. Portell Bueso,¹² S. Pospisil,¹²⁷ K. Potamianos,¹⁵ I. N. Potrap,⁶⁴ C. J. Potter,¹⁵⁰ C. T. Potter,¹¹⁵ G. Poulard,³⁰ J. Poveda,⁶⁰ V. Pozdnyakov,⁶⁴ P. Pralavorio,⁸⁴ A. Pranko,¹⁵ S. Prasad,³⁰ R. Pravahan,⁸ S. Prell,⁶³ D. Price,⁸³ J. Price,⁷³ L. E. Price,⁶ D. Prieur,¹²⁴ M. Primavera,^{72a} M. Proissl,⁴⁶ K. Prokofiev,⁴⁷ F. Prokoshin,^{32b} E. Protopapadaki,¹³⁷ S. Protopopescu,²⁵ J. Proudfoot,⁶ M. Przybycien,^{38a} H. Przysiezniaik,⁵ E. Ptacek,¹¹⁵ D. Puddu,^{135a,135b} E. Pueschel,⁸⁵ D. Puldon,¹⁴⁹ M. Purohit,^{25,ee} P. Puzo,¹¹⁶ J. Qian,⁸⁸ G. Qin,⁵³ Y. Qin,⁸³ A. Quadt,⁵⁴ D. R. Quarrie,¹⁵ W. B. Quayle,^{165a,165b} M. Queitsch-Maitland,⁸³ D. Quilty,⁵³ A. Qureshi,^{160b} V. Radeka,²⁵ V. Radescu,⁴² S. K. Radhakrishnan,¹⁴⁹ P. Radloff,¹¹⁵ P. Rados,⁸⁷ F. Ragusa,^{90a,90b} G. Rahal,¹⁷⁹ S. Rajagopalan,²⁵ M. Rammensee,³⁰ A. S. Randle-Conde,⁴⁰ C. Rangel-Smith,¹⁶⁷ K. Rao,¹⁶⁴ F. Rauscher,⁹⁹ T. C. Rave,⁴⁸ T. Ravenscroft,⁵³ M. Raymond,³⁰ A. L. Read,¹¹⁸ N. P. Readioff,⁷³ D. M. Rebuffi,^{120a,120b} A. Redelbach,¹⁷⁵ G. Redlinger,²⁵ R. Reece,¹³⁸ K. Reeves,⁴¹ L. Rehnisch,¹⁶ H. Reisin,²⁷ M. Relich,¹⁶⁴ C. Rembser,³⁰ H. Ren,^{33a} Z. L. Ren,¹⁵² A. Renaud,¹¹⁶ M. Rescigno,^{133a} S. Resconi,^{90a} O. L. Rezanova,^{108,u} P. Reznicek,¹²⁸ R. Rezvani,⁹⁴ R. Richter,¹⁰⁰ M. Ridel,⁷⁹ P. Rieck,¹⁶ J. Rieger,⁵⁴ M. Rijssenbeek,¹⁴⁹ A. Rimoldi,^{120a,120b} L. Rinaldi,^{20a} E. Ritsch,⁶¹ I. Riu,¹² F. Rizatdinova,¹¹³ E. Rizvi,⁷⁵ S. H. Robertson,^{86,j} A. Robichaud-Veronneau,⁸⁶ D. Robinson,²⁸ J. E. M. Robinson,⁸³ A. Robson,⁵³ C. Roda,^{123a,123b} L. Rodrigues,³⁰ S. Roe,³⁰ O. Røhne,¹¹⁸ S. Rolli,¹⁶² A. Romaniouk,⁹⁷ M. Romano,^{20a,20b} E. Romero Adam,¹⁶⁸ N. Rompotis,¹³⁹ M. Ronzani,⁴⁸ L. Roos,⁷⁹ E. Ros,¹⁶⁸ S. Rosati,^{133a} K. Rosbach,⁴⁹ M. Rose,⁷⁶ P. Rose,¹³⁸ P. L. Rosendahl,¹⁴ O. Rosenthal,¹⁴² V. Rossetti,^{147a,147b} E. Rossi,^{103a,103b} L. P. Rossi,^{50a} R. Rosten,¹³⁹ M. Rotaru,^{26a} I. Roth,¹⁷³ J. Rothberg,¹³⁹ D. Rousseau,¹¹⁶ C. R. Royon,¹³⁷ A. Rozanov,⁸⁴ Y. Rozen,¹⁵³ X. Ruan,^{146c} F. Rubbo,¹² I. Rubinskiy,⁴² V. I. Rud,⁹⁸ C. Rudolph,⁴⁴ M. S. Rudolph,¹⁵⁹ F. Rühr,⁴⁸ A. Ruiz-Martinez,³⁰ Z. Rurikova,⁴⁸

N. A. Rusakovich,⁶⁴ A. Ruschke,⁹⁹ J. P. Rutherford,⁷ N. Ruthmann,⁴⁸ Y. F. Ryabov,¹²² M. Rybar,¹²⁸ G. Rybkin,¹¹⁶ N. C. Ryder,¹¹⁹ A. F. Saavedra,¹⁵¹ S. Sacerdoti,²⁷ A. Saddique,³ I. Sadeh,¹⁵⁴ H. F.-W. Sadrozinski,¹³⁸ R. Sadykov,⁶⁴ F. Safai Tehrani,^{133a} H. Sakamoto,¹⁵⁶ Y. Sakurai,¹⁷² G. Salamanna,^{135a,135b} A. Salamon,^{134a} M. Saleem,¹¹² D. Salek,¹⁰⁶ P. H. Sales De Bruin,¹³⁹ D. Salihagic,¹⁰⁰ A. Salnikov,¹⁴⁴ J. Salt,¹⁶⁸ D. Salvatore,^{37a,37b} F. Salvatore,¹⁵⁰ A. Salvucci,¹⁰⁵ A. Salzburger,³⁰ D. Sampsonidis,¹⁵⁵ A. Sanchez,^{103a,103b} J. Sánchez,¹⁶⁸ V. Sanchez Martinez,¹⁶⁸ H. Sandaker,¹⁴ R. L. Sandbach,⁷⁵ H. G. Sander,⁸² M. P. Sanders,⁹⁹ M. Sandhoff,¹⁷⁶ T. Sandoval,²⁸ C. Sandoval,¹⁶³ R. Sandstroem,¹⁰⁰ D. P. C. Sankey,¹³⁰ A. Sansoni,⁴⁷ C. Santoni,³⁴ R. Santonico,^{134a,134b} H. Santos,^{125a} I. Santoyo Castillo,¹⁵⁰ K. Sapp,¹²⁴ A. Saprosov,⁶⁴ J. G. Saraiva,^{125a,125d} B. Sarrazin,²¹ G. Sartisohn,¹⁷⁶ O. Sasaki,⁶⁵ Y. Sasaki,¹⁵⁶ G. Sauvage,^{5a} E. Sauvan,⁵ P. Savard,^{159,e} D. O. Savu,³⁰ C. Sawyer,¹¹⁹ L. Sawyer,^{78,n} D. H. Saxon,⁵³ J. Saxon,¹²¹ C. Sbarra,^{20a} A. Sbrizzi,³ T. Scanlon,⁷⁷ D. A. Scannicchio,¹⁶⁴ M. Scarcella,¹⁵¹ V. Scarfone,^{37a,37b} J. Schaarschmidt,¹⁷³ P. Schacht,¹⁰⁰ D. Schaefer,³⁰ R. Schaefer,⁴² S. Schaepe,²¹ S. Schaetzel,^{58b} U. Schäfer,⁸² A. C. Schaffer,¹¹⁶ D. Schaile,⁹⁹ R. D. Schamberger,¹⁴⁹ V. Scharf,^{58a} V. A. Schegelsky,¹²² D. Scheirich,¹²⁸ M. Schernau,¹⁶⁴ M. I. Scherzer,³⁵ C. Schiavi,^{50a,50b} J. Schieck,⁹⁹ C. Schillo,⁴⁸ M. Schioppa,^{37a,37b} S. Schlenker,³⁰ E. Schmidt,⁴⁸ K. Schmieden,³⁰ C. Schmitt,⁸² S. Schmitt,^{58b} B. Schneider,¹⁷ Y. J. Schnellbach,⁷³ U. Schnoor,⁴⁴ L. Schoeffel,¹³⁷ A. Schoening,^{58b} B. D. Schoenrock,⁸⁹ A. L. S. Schorlemmer,⁵⁴ M. Schott,⁸² D. Schouten,^{160a} J. Schovancova,²⁵ S. Schramm,¹⁵⁹ M. Schreyer,¹⁷⁵ C. Schroeder,⁸² N. Schuh,⁸² M. J. Schultens,²¹ H.-C. Schultz-Coulon,^{58a} H. Schulz,¹⁶ M. Schumacher,⁴⁸ B. A. Schumm,¹³⁸ Ph. Schune,¹³⁷ C. Schwanenberger,⁸³ A. Schwartzman,¹⁴⁴ T. A. Schwarz,⁸⁸ Ph. Schwegler,¹⁰⁰ Ph. Schwemling,¹³⁷ R. Schwienhorst,⁸⁹ J. Schwindling,¹³⁷ T. Schwindt,²¹ M. Schwoerer,⁵ F. G. Sciacca,¹⁷ E. Scifo,¹¹⁶ G. Sciolla,²³ W. G. Scott,¹³⁰ F. Scuri,^{123a,123b} F. Scutti,²¹ J. Searcy,⁸⁸ G. Sedov,⁴² E. Sedykh,¹²² S. C. Seidel,¹⁰⁴ A. Seiden,¹³⁸ F. Seifert,¹²⁷ J. M. Seixas,^{24a} G. Sekhniaidze,^{103a} S. J. Sekula,⁴⁰ K. E. Selbach,⁴⁶ D. M. Seliverstov,^{122,a} G. Sellers,⁷³ N. Semprini-Cesari,^{20a,20b} C. Serfon,³⁰ L. Serin,¹¹⁶ L. Serkin,⁵⁴ T. Serre,⁸⁴ R. Seuster,^{160a} H. Severini,¹¹² T. Sfiligoi,⁷⁴ F. Sforza,¹⁰⁰ A. Sfyrla,³⁰ E. Shabalina,⁵⁴ M. Shamim,¹¹⁵ L. Y. Shan,^{33a} R. Shang,¹⁶⁶ J. T. Shank,²² M. Shapiro,¹⁵ P. B. Shatalov,⁹⁶ K. Shaw,^{165a,165b} C. Y. Shehu,¹⁵⁰ P. Sherwood,⁷⁷ L. Shi,^{152,ff} S. Shimizu,⁶⁶ C. O. Shimmin,¹⁶⁴ M. Shimojima,¹⁰¹ M. Shiyakova,⁶⁴ A. Shmeleva,⁹⁵ M. J. Shochet,³¹ D. Short,¹¹⁹ S. Shrestha,⁶³ E. Shulga,⁹⁷ M. A. Shupe,⁷ S. Shushkevich,⁴² P. Sicho,¹²⁶ O. Sidiropoulou,¹⁵⁵ D. Sidorov,¹¹³ A. Sidoti,^{133a} F. Siegert,⁴⁴ Dj. Sijacki,^{13a} J. Silva,^{125a,125d} Y. Silver,¹⁵⁴ D. Silverstein,¹⁴⁴ S. B. Silverstein,^{147a} V. Simak,¹²⁷ O. Simard,⁵ Lj. Simic,^{13a} S. Simion,¹¹⁶ E. Simioni,⁸² B. Simmons,⁷⁷ R. Simoniello,^{90a,90b} M. Simonyan,³⁶ P. Sinervo,¹⁵⁹ N. B. Sinev,¹¹⁵ V. Sipica,¹⁴² G. Siragusa,¹⁷⁵ A. Sircar,⁷⁸ A. N. Sisakyan,^{64,a} S. Yu. Sivoklokov,⁹⁸ J. Sjölin,^{147a,147b} T. B. Sjurson,¹⁴ H. P. Skottowe,⁵⁷ K. Yu. Skovpen,¹⁰⁸ P. Skubic,¹¹² M. Slater,¹⁸ T. Slavicek,¹²⁷ K. Sliwa,¹⁶² V. Smakhtin,¹⁷³ B. H. Smart,⁴⁶ L. Smestad,¹⁴ S. Yu. Smirnov,⁹⁷ Y. Smirnov,⁹⁷ L. N. Smirnova,^{98,gg} O. Smirnova,⁸⁰ K. M. Smith,⁵³ M. Smizanska,⁷¹ K. Smolek,¹²⁷ A. A. Snesarev,⁹⁵ G. Snidero,⁷⁵ S. Snyder,²⁵ R. Sobie,^{170,j} F. Socher,⁴⁴ A. Soffer,¹⁵⁴ D. A. Soh,^{152,ff} C. A. Solans,³⁰ M. Solar,¹²⁷ J. Solc,¹²⁷ E. Yu. Soldatov,⁹⁷ U. Soldevila,¹⁶⁸ A. A. Solodkov,¹²⁹ A. Soloshenko,⁶⁴ O. V. Solovyanov,¹²⁹ V. Solovyev,¹²² P. Sommer,⁴⁸ H. Y. Song,^{33b} N. Soni,¹ A. Sood,¹⁵ A. Sopczak,¹²⁷ B. Sopko,¹²⁷ V. Sopko,¹²⁷ V. Sorin,¹² M. Sosebee,⁸ R. Soualah,^{165a,165c} P. Soueid,⁹⁴ A. M. Soukharev,¹⁰⁸ D. South,⁴² S. Spagnolo,^{72a,72b} F. Spanò,⁷⁶ W. R. Spearman,⁵⁷ F. Spettel,¹⁰⁰ R. Spighi,^{20a} G. Spigo,³⁰ L. A. Spiller,⁸⁷ M. Spousta,¹²⁸ T. Spreitzer,¹⁵⁹ B. Spurlock,⁸ R. D. St. Denis,^{53,a} S. Staerz,⁴⁴ J. Stahlman,¹²¹ R. Stamen,^{58a} S. Stamm,¹⁶ E. Stanecka,³⁹ R. W. Stanek,⁶ C. Stanescu,^{135a} M. Stanescu-Bellu,⁴² M. M. Stanitzki,⁴² S. Stapnes,¹¹⁸ E. A. Starchenko,¹²⁹ J. Stark,⁵⁵ P. Staroba,¹²⁶ P. Starovoitov,⁴² R. Staszewski,³⁹ P. Stavina,^{145a,a} P. Steinberg,²⁵ B. Stelzer,¹⁴³ H. J. Stelzer,³⁰ O. Stelzer-Chilton,^{160a} H. Stenzel,⁵² S. Stern,¹⁰⁰ G. A. Stewart,⁵³ J. A. Stillings,²¹ M. C. Stockton,⁸⁶ M. Stoebe,⁸⁶ G. Stoicea,^{26a} P. Stolte,⁵⁴ S. Stonjek,¹⁰⁰ A. R. Stradling,⁸ A. Straessner,⁴⁴ M. E. Stramaglia,¹⁷ J. Strandberg,¹⁴⁸ S. Strandberg,^{147a,147b} A. Strandlie,¹¹⁸ E. Strauss,¹⁴⁴ M. Strauss,¹¹² P. Strizenec,^{145b} R. Ströhmer,¹⁷⁵ D. M. Strom,¹¹⁵ R. Stroynowski,⁴⁰ A. Struebig,¹⁰⁵ S. A. Stucci,¹⁷ B. Stugu,¹⁴ N. A. Styles,⁴² D. Su,¹⁴⁴ J. Su,¹²⁴ R. Subramaniam,⁷⁸ A. Succurro,¹² Y. Sugaya,¹¹⁷ C. Suhr,¹⁰⁷ M. Suk,¹²⁷ V. V. Sulin,⁹⁵ S. Sultansoy,^{4c} T. Sumida,⁶⁷ S. Sun,⁵⁷ X. Sun,^{33a} J. E. Sundermann,⁴⁸ K. Suruliz,¹⁴⁰ G. Susinno,^{37a,37b} M. R. Sutton,¹⁵⁰ Y. Suzuki,⁶⁵ M. Svatos,¹²⁶ S. Swedish,¹⁶⁹ M. Swiatlowski,¹⁴⁴ I. Sykora,^{145a} T. Sykora,¹²⁸ D. Ta,⁸⁹ C. Taccini,^{135a,135b} K. Tackmann,⁴² J. Taenzer,¹⁵⁹ A. Taffard,¹⁶⁴ R. Tafirout,^{160a} N. Taiblum,¹⁵⁴ H. Takai,²⁵ R. Takashima,⁶⁸ H. Takeda,⁶⁶ T. Takeshita,¹⁴¹ Y. Takubo,⁶⁵ M. Talby,⁸⁴ A. A. Talyshiev,^{108,u} J. Y. C. Tam,¹⁷⁵ K. G. Tan,⁸⁷ J. Tanaka,¹⁵⁶ R. Tanaka,¹¹⁶ S. Tanaka,¹³² S. Tanaka,⁶⁵ A. J. Tanasijczuk,¹⁴³ B. B. Tannenwald,¹¹⁰ N. Tannoury,²¹ S. Tapprogge,⁸² S. Tarem,¹⁵³ F. Tarrade,²⁹ G. F. Tartarelli,^{90a} P. Tas,¹²⁸ M. Tasevsky,¹²⁶ T. Tashiro,⁶⁷ E. Tassi,^{37a,37b} A. Tavares Delgado,^{125a,125b} Y. Tayalati,^{136d} F. E. Taylor,⁹³ G. N. Taylor,⁸⁷ W. Taylor,^{160b} F. A. Teischinger,³⁰ M. Teixeira Dias Castanheira,⁷⁵ P. Teixeira-Dias,⁷⁶ K. K. Temming,⁴⁸ H. Ten Kate,³⁰ P. K. Teng,¹⁵²

J. J. Teoh,¹¹⁷ S. Terada,⁶⁵ K. Terashi,¹⁵⁶ J. Terron,⁸¹ S. Terzo,¹⁰⁰ M. Testa,⁴⁷ R. J. Teuscher,^{159j} J. Therhaag,²¹
T. Theveneaux-Pelzer,³⁴ J. P. Thomas,¹⁸ J. Thomas-Wilsker,⁷⁶ E. N. Thompson,³⁵ P. D. Thompson,¹⁸ P. D. Thompson,¹⁵⁹
R. J. Thompson,⁸³ A. S. Thompson,⁵³ L. A. Thomsen,³⁶ E. Thomson,¹²¹ M. Thomson,²⁸ W. M. Thong,⁸⁷ R. P. Thun,^{88,a}
F. Tian,³⁵ M. J. Tibbetts,¹⁵ V. O. Tikhomirov,^{95,hh} Yu. A. Tikhonov,^{108,u} S. Timoshenko,⁹⁷ E. Tiouchichine,⁸⁴ P. Tipton,¹⁷⁷
S. Tisserant,⁸⁴ T. Todorov,⁵ S. Todorova-Nova,¹²⁸ B. Toggerson,⁷ J. Tojo,⁶⁹ S. Tokár,^{145a} K. Tokushuku,⁶⁵ K. Tollefson,⁸⁹
L. Tomlinson,⁸³ M. Tomoto,¹⁰² L. Tompkins,³¹ K. Toms,¹⁰⁴ N. D. Topilin,⁶⁴ E. Torrence,¹¹⁵ H. Torres,¹⁴³ E. Torró Pastor,¹⁶⁸
J. Toth,^{84,ii} F. Touchard,⁸⁴ D. R. Tovey,¹⁴⁰ H. L. Tran,¹¹⁶ T. Trefzger,¹⁷⁵ L. Tremblet,³⁰ A. Tricoli,³⁰ I. M. Trigger,^{160a}
S. Trincaz-Duvoid,⁷⁹ M. F. Tripania,¹² W. Trischuk,¹⁵⁹ B. Trocmé,⁵⁵ C. Troncon,^{90a} M. Trottier-McDonald,¹⁵
M. Trovatelli,^{135a,135b} P. True,⁸⁹ M. Trzebinski,³⁹ A. Trzupek,³⁹ C. Tsarouchas,³⁰ J. C-L. Tseng,¹¹⁹ P. V. Tsiareshka,⁹¹
D. Tsionou,¹³⁷ G. Tsipolitis,¹⁰ N. Tsirintanis,⁹ S. Tsiskaridze,¹² V. Tsiskaridze,⁴⁸ E. G. Tskhadadze,^{51a} I. I. Tsukerman,⁹⁶
V. Tsulaia,¹⁵ S. Tsuno,⁶⁵ D. Tsybychev,¹⁴⁹ A. Tudorache,^{26a} V. Tudorache,^{26a} A. N. Tuna,¹²¹ S. A. Tuppiti,^{20a,20b}
S. Turchikhin,^{98,gg} D. Turecek,¹²⁷ I. Turk Cakir,^{4d} R. Turra,^{90a,90b} P. M. Tuts,³⁵ A. Tykhonov,⁴⁹ M. Tylmad,^{147a,147b}
M. Tyndel,¹³⁰ K. Uchida,²¹ I. Ueda,¹⁵⁶ R. Ueno,²⁹ M. Ughetto,⁸⁴ M. Ugland,¹⁴ M. Uhlenbrock,²¹ F. Ukegawa,¹⁶¹ G. Unal,³⁰
A. Undrus,²⁵ G. Unel,¹⁶⁴ F. C. Ungaro,⁴⁸ Y. Unno,⁶⁵ C. Unverdorben,⁹⁹ D. Urbaniec,³⁵ P. Urquijo,⁸⁷ G. Usai,⁸ A. Usanova,⁶¹
L. Vacavant,⁸⁴ V. Vacek,¹²⁷ B. Vachon,⁸⁶ N. Valencic,¹⁰⁶ S. Valentinetti,^{20a,20b} A. Valero,¹⁶⁸ L. Valery,³⁴ S. Valkar,¹²⁸
E. Valladolid Gallego,¹⁶⁸ S. Vallecorsa,⁴⁹ J. A. Valls Ferrer,¹⁶⁸ W. Van Den Wollenberg,¹⁰⁶ P. C. Van Der Deijl,¹⁰⁶
R. van der Geer,¹⁰⁶ H. van der Graaf,¹⁰⁶ R. Van Der Leeuw,¹⁰⁶ D. van der Ster,³⁰ N. van Eldik,³⁰ P. van Gemmeren,⁶
J. Van Nieuwkoop,¹⁴³ I. van Vulpen,¹⁰⁶ M. C. van Woerden,³⁰ M. Vanadia,^{133a,133b} W. Vandelli,³⁰ R. Vanguri,¹²¹
A. Vaniachine,⁶ P. Vankov,⁴² F. Vannucci,⁷⁹ G. Vardanyan,¹⁷⁸ R. Vari,^{133a} E. W. Varnes,⁷ T. Varol,⁸⁵ D. Varouchas,⁷⁹
A. Vartapetian,⁸ K. E. Varvell,¹⁵¹ F. Vazeille,³⁴ T. Vazquez Schroeder,⁵⁴ J. Veatch,⁷ F. Veloso,^{125a,125c} S. Veneziano,^{133a}
A. Ventura,^{72a,72b} D. Ventura,⁸⁵ M. Venturi,¹⁷⁰ N. Venturi,¹⁵⁹ A. Venturini,²³ V. Vercesi,^{120a} M. Verducci,^{133a,133b}
W. Verkerke,¹⁰⁶ J. C. Vermeulen,¹⁰⁶ A. Vest,⁴⁴ M. C. Vetterli,^{143,e} O. Viazlo,⁸⁰ I. Vichou,¹⁶⁶ T. Vickey,^{146c,jj}
O. E. Vickey Boeriu,^{146c} G. H. A. Viehhauser,¹¹⁹ S. Viel,¹⁶⁹ R. Vigne,³⁰ M. Villa,^{20a,20b} M. Villaplana Perez,^{90a,90b}
E. Vilucchi,⁴⁷ M. G. Vinciter,²⁹ V. B. Vinogradov,⁶⁴ J. Virzi,¹⁵ I. Vivarelli,¹⁵⁰ F. Vives Vaque,³ S. Vlachos,¹⁰ D. Vladoiu,⁹⁹
M. Vlasak,¹²⁷ A. Vogel,²¹ M. Vogel,^{32a} P. Vokac,¹²⁷ G. Volpi,^{123a,123b} M. Volpi,⁸⁷ H. von der Schmitt,¹⁰⁰ H. von Radziewski,⁴⁸
E. von Toerne,²¹ V. Vorobel,¹²⁸ K. Vorobev,⁹⁷ M. Vos,¹⁶⁸ R. Voss,³⁰ J. H. Vosseveld,⁷³ N. Vranjes,¹³⁷
M. Vranjes Milosavljevic,^{13a} V. Vrba,¹²⁶ M. Vreeswijk,¹⁰⁶ T. Vu Anh,⁴⁸ R. Vuillermet,³⁰ I. Vukotic,³¹ Z. Vykydal,¹²⁷
P. Wagner,²¹ W. Wagner,¹⁷⁶ H. Wahlberg,⁷⁰ S. Wahrmund,⁴⁴ J. Wakabayashi,¹⁰² J. Walder,⁷¹ R. Walker,⁹⁹ W. Walkowiak,¹⁴²
R. Wall,¹⁷⁷ P. Waller,⁷³ B. Walsh,¹⁷⁷ C. Wang,^{152,kk} C. Wang,⁴⁵ F. Wang,¹⁷⁴ H. Wang,¹⁵ H. Wang,⁴⁰ J. Wang,⁴² J. Wang,^{33a}
K. Wang,⁸⁶ R. Wang,¹⁰⁴ S. M. Wang,¹⁵² T. Wang,²¹ X. Wang,¹⁷⁷ C. Wanotayaroj,¹¹⁵ A. Warburton,⁸⁶ C. P. Ward,²⁸
D. R. Wardrope,⁷⁷ M. Warsinsky,⁴⁸ A. Washbrook,⁴⁶ C. Wasicki,⁴² P. M. Watkins,¹⁸ A. T. Watson,¹⁸ I. J. Watson,¹⁵¹
M. F. Watson,¹⁸ G. Watts,¹³⁹ S. Watts,⁸³ B. M. Waugh,⁷⁷ S. Webb,⁸³ M. S. Weber,¹⁷ S. W. Weber,¹⁷⁵ J. S. Webster,³¹
A. R. Weidberg,¹¹⁹ P. Weigell,¹⁰⁰ B. Weinert,⁶⁰ J. Weingarten,⁵⁴ C. Weiser,⁴⁸ H. Weits,¹⁰⁶ P. S. Wells,³⁰ T. Wenaus,²⁵
D. Wendland,¹⁶ Z. Weng,^{152,ff} T. Wengler,³⁰ S. Wenig,³⁰ N. Wermes,²¹ M. Werner,⁴⁸ P. Werner,³⁰ M. Wessels,^{58a} J. Wetter,¹⁶²
K. Whalen,²⁹ A. White,⁸ M. J. White,¹ R. White,^{32b} S. White,^{123a,123b} D. Whiteson,¹⁶⁴ D. Wicke,¹⁷⁶ F. J. Wickens,¹³⁰
W. Wiedenmann,¹⁷⁴ M. Wielers,¹³⁰ P. Wienemann,²¹ C. Wiglesworth,³⁶ L. A. M. Wiik-Fuchs,²¹ P. A. Wijeratne,⁷⁷
A. Wildauer,¹⁰⁰ M. A. Wildt,^{42,ll} H. G. Wilkens,³⁰ J. Z. Will,⁹⁹ H. H. Williams,¹²¹ S. Williams,²⁸ C. Willis,⁸⁹ S. Willocq,⁸⁵
A. Wilson,⁸⁸ J. A. Wilson,¹⁸ I. Wingerter-Seez,⁵ F. Winklmeier,¹¹⁵ B. T. Winter,²¹ M. Wittgen,¹⁴⁴ T. Wittig,⁴³
J. Wittkowski,⁹⁹ S. J. Wollstadt,⁸² M. W. Wolter,³⁹ H. Wolters,^{125a,125c} B. K. Wosiek,³⁹ J. Wotschack,³⁰ M. J. Woudstra,⁸³
K. W. Wozniak,³⁹ M. Wright,⁵³ M. Wu,⁵⁵ S. L. Wu,¹⁷⁴ X. Wu,⁴⁹ Y. Wu,⁸⁸ E. Wulf,³⁵ T. R. Wyatt,⁸³ B. M. Wynne,⁴⁶
S. Xella,³⁶ M. Xiao,¹³⁷ D. Xu,^{33a} L. Xu,^{33b,mmm} B. Yabsley,¹⁵¹ S. Yacoub,^{146b,nn} R. Yakabe,⁶⁶ M. Yamada,⁶⁵ H. Yamaguchi,¹⁵⁶
Y. Yamaguchi,¹¹⁷ A. Yamamoto,⁶⁵ K. Yamamoto,⁶³ S. Yamamoto,¹⁵⁶ T. Yamamura,¹⁵⁶ T. Yamanaka,¹⁵⁶ K. Yamauchi,¹⁰²
Y. Yamazaki,⁶⁶ Z. Yan,²² H. Yang,^{33e} H. Yang,¹⁷⁴ U. K. Yang,⁸³ Y. Yang,¹¹⁰ S. Yanush,⁹² L. Yao,^{33a} W-M. Yao,¹⁵ Y. Yasu,⁶⁵
E. Yatsenko,⁴² K. H. Yau Wong,²¹ J. Ye,⁴⁰ S. Ye,²⁵ I. Yeletsikh,⁶⁴ A. L. Yen,⁵⁷ E. Yildirim,⁴² M. Yilmaz,^{4b}
R. Yoosofmiya,¹²⁴ K. Yorita,¹⁷² R. Yoshida,⁶ K. Yoshihara,¹⁵⁶ C. Young,¹⁴⁴ C. J. S. Young,³⁰ S. Youssef,²² D. R. Yu,¹⁵
J. Yu,⁸ J. M. Yu,⁸⁸ J. Yu,¹¹³ L. Yuan,⁶⁶ A. Yurkewicz,¹⁰⁷ I. Yusuff,^{28,oo} B. Zabinski,³⁹ R. Zaidan,⁶² A. M. Zaitsev,^{129,bb}
A. Zaman,¹⁴⁹ S. Zambito,²³ L. Zanello,^{133a,133b} D. Zanzi,¹⁰⁰ C. Zeitnitz,¹⁷⁶ M. Zeman,¹²⁷ A. Zemla,^{38a} K. Zengel,²³
O. Zenin,¹²⁹ T. Ženiš,^{145a} D. Zerwas,¹¹⁶ G. Zevi della Porta,⁵⁷ D. Zhang,⁸⁸ F. Zhang,¹⁷⁴ H. Zhang,⁸⁹ J. Zhang,⁶ L. Zhang,¹⁵²
X. Zhang,^{33d} Z. Zhang,¹¹⁶ Z. Zhao,^{33b} A. Zhemchugov,⁶⁴ J. Zhong,¹¹⁹ B. Zhou,⁸⁸ L. Zhou,³⁵ N. Zhou,¹⁶⁴ C. G. Zhu,^{33d}

H. Zhu,^{33a} J. Zhu,⁸⁸ Y. Zhu,^{33b} X. Zhuang,^{33a} K. Zhukov,⁹⁵ A. Zibell,¹⁷⁵ D. Zieminska,⁶⁰ N. I. Zimine,⁶⁴ C. Zimmermann,⁸²
 R. Zimmermann,²¹ S. Zimmermann,²¹ S. Zimmermann,⁴⁸ Z. Zinonos,⁵⁴ M. Ziolkowski,¹⁴² G. Zobernig,¹⁷⁴ A. Zoccoli,^{20a,20b}
 M. zur Nedden,¹⁶ G. Zurzolo,^{103a,103b} V. Zutshi,¹⁰⁷ and L. Zwalinski³⁰

(ATLAS Collaboration)

- ¹*Department of Physics, University of Adelaide, Adelaide, Australia*
²*Physics Department, SUNY Albany, Albany, New York, USA*
³*Department of Physics, University of Alberta, Edmonton, Alberta, Canada*
^{4a}*Department of Physics, Ankara University, Ankara, Turkey*
^{4b}*Department of Physics, Gazi University, Ankara, Turkey*
^{4c}*Division of Physics, TOBB University of Economics and Technology, Ankara, Turkey*
^{4d}*Turkish Atomic Energy Authority, Ankara, Turkey*
⁵*LAPP, CNRS/IN2P3 and Université de Savoie, Annecy-le-Vieux, France*
⁶*High Energy Physics Division, Argonne National Laboratory, Argonne IL, USA*
⁷*Department of Physics, University of Arizona, Tucson, Arizona, USA*
⁸*Department of Physics, The University of Texas at Arlington, Arlington, Texas, USA*
⁹*Physics Department, University of Athens, Athens, Greece*
¹⁰*Physics Department, National Technical University of Athens, Zografou, Greece*
¹¹*Institute of Physics, Azerbaijan Academy of Sciences, Baku, Azerbaijan*
¹²*Institut de Física d'Altes Energies and Departament de Física de la Universitat Autònoma de Barcelona, Barcelona, Spain*
^{13a}*Institute of Physics, University of Belgrade, Belgrade, Serbia*
^{13b}*Vinca Institute of Nuclear Sciences, University of Belgrade, Belgrade, Serbia*
¹⁴*Department for Physics and Technology, University of Bergen, Bergen, Norway*
¹⁵*Physics Division, Lawrence Berkeley National Laboratory and University of California, Berkeley, California, USA*
¹⁶*Department of Physics, Humboldt University, Berlin, Germany*
¹⁷*Albert Einstein Center for Fundamental Physics and Laboratory for High Energy Physics, University of Bern, Bern, Switzerland*
¹⁸*School of Physics and Astronomy, University of Birmingham, Birmingham, United Kingdom*
^{19a}*Department of Physics, Bogazici University, Istanbul, Turkey*
^{19b}*Department of Physics, Dogus University, Istanbul, Turkey*
^{19c}*Department of Physics Engineering, Gaziantep University, Gaziantep, Turkey*
^{20a}*INFN Sezione di Bologna, Italy*
^{20b}*Dipartimento di Fisica e Astronomia, Università di Bologna, Bologna, Italy*
²¹*Physikalisches Institut, University of Bonn, Bonn, Germany*
²²*Department of Physics, Boston University, Boston, Massachusetts, USA*
²³*Department of Physics, Brandeis University, Waltham, Massachusetts, USA*
^{24a}*Universidade Federal do Rio De Janeiro COPPE/EE/IF, Rio de Janeiro, Brazil*
^{24b}*Federal University of Juiz de Fora (UFJF), Juiz de Fora, Brazil*
^{24c}*Federal University of Sao Joao del Rei (UFSJ), Sao Joao del Rei, Brazil*
^{24d}*Instituto de Física, Universidade de Sao Paulo, Sao Paulo, Brazil*
²⁵*Physics Department, Brookhaven National Laboratory, Upton, New York, USA*
^{26a}*National Institute of Physics and Nuclear Engineering, Bucharest, Romania*
^{26b}*National Institute for Research and Development of Isotopic and Molecular Technologies, Physics Department, Cluj Napoca, Romania*
^{26c}*University Politehnica Bucharest, Bucharest, Romania*
^{26d}*West University in Timisoara, Timisoara, Romania*
²⁷*Departamento de Física, Universidad de Buenos Aires, Buenos Aires, Argentina*
²⁸*Cavendish Laboratory, University of Cambridge, Cambridge, United Kingdom*
²⁹*Department of Physics, Carleton University, Ottawa, Ontario, Canada*
³⁰*CERN, Geneva, Switzerland*
³¹*Enrico Fermi Institute, University of Chicago, Chicago, Illinois, USA*
^{32a}*Departamento de Física, Pontificia Universidad Católica de Chile, Santiago, Chile*
^{32b}*Departamento de Física, Universidad Técnica Federico Santa María, Valparaíso, Chile*
^{33a}*Institute of High Energy Physics, Chinese Academy of Sciences, Beijing, China*
^{33b}*Department of Modern Physics, University of Science and Technology of China, Anhui, China*
^{33c}*Department of Physics, Nanjing University, Jiangsu, China*

- ^{33d}*School of Physics, Shandong University, Shandong, China*
- ^{33e}*Physics Department, Shanghai Jiao Tong University, Shanghai, China*
- ³⁴*Laboratoire de Physique Corpusculaire, Clermont Université and Université Blaise Pascal and CNRS/IN2P3, Clermont-Ferrand, France*
- ³⁵*Nevis Laboratory, Columbia University, Irvington, New York, USA*
- ³⁶*Niels Bohr Institute, University of Copenhagen, Kobenhavn, Denmark*
- ^{37a}*INFN Gruppo Collegato di Cosenza, Laboratori Nazionali di Frascati, Italy*
- ^{37b}*Dipartimento di Fisica, Università della Calabria, Rende, Italy*
- ^{38a}*AGH University of Science and Technology, Faculty of Physics and Applied Computer Science, Krakow, Poland*
- ^{38b}*Marian Smoluchowski Institute of Physics, Jagiellonian University, Krakow, Poland*
- ³⁹*The Henryk Niewodniczanski Institute of Nuclear Physics, Polish Academy of Sciences, Krakow, Poland*
- ⁴⁰*Physics Department, Southern Methodist University, Dallas, Texas, USA*
- ⁴¹*Physics Department, University of Texas at Dallas, Richardson, Texas, USA*
- ⁴²*DESY, Hamburg and Zeuthen, Germany*
- ⁴³*Institut für Experimentelle Physik IV, Technische Universität Dortmund, Dortmund, Germany*
- ⁴⁴*Institut für Kern- und Teilchenphysik, Technische Universität Dresden, Dresden, Germany*
- ⁴⁵*Department of Physics, Duke University, Durham, North Carolina, USA*
- ⁴⁶*SUPA-School of Physics and Astronomy, University of Edinburgh, Edinburgh, United Kingdom*
- ⁴⁷*INFN Laboratori Nazionali di Frascati, Frascati, Italy*
- ⁴⁸*Fakultät für Mathematik und Physik, Albert-Ludwigs-Universität, Freiburg, Germany*
- ⁴⁹*Section de Physique, Université de Genève, Geneva, Switzerland*
- ^{50a}*INFN Sezione di Genova, Italy*
- ^{50b}*Dipartimento di Fisica, Università di Genova, Genova, Italy*
- ^{51a}*E. Andronikashvili Institute of Physics, Iv. Javakishvili Tbilisi State University, Tbilisi, Georgia*
- ^{51b}*High Energy Physics Institute, Tbilisi State University, Tbilisi, Georgia*
- ⁵²*II Physikalisches Institut, Justus-Liebig-Universität Giessen, Giessen, Germany*
- ⁵³*SUPA-School of Physics and Astronomy, University of Glasgow, Glasgow, United Kingdom*
- ⁵⁴*II Physikalisches Institut, Georg-August-Universität, Göttingen, Germany*
- ⁵⁵*Laboratoire de Physique Subatomique et de Cosmologie, Université Grenoble-Alpes, CNRS/IN2P3, Grenoble, France*
- ⁵⁶*Department of Physics, Hampton University, Hampton, Virginia, USA*
- ⁵⁷*Laboratory for Particle Physics and Cosmology, Harvard University, Cambridge, Massachusetts, USA*
- ^{58a}*Kirchhoff-Institut für Physik, Ruprecht-Karls-Universität Heidelberg, Heidelberg, Germany*
- ^{58b}*Physikalisches Institut, Ruprecht-Karls-Universität Heidelberg, Heidelberg, Germany*
- ^{58c}*ZITI Institut für technische Informatik, Ruprecht-Karls-Universität Heidelberg, Mannheim, Germany*
- ⁵⁹*Faculty of Applied Information Science, Hiroshima Institute of Technology, Hiroshima, Japan*
- ⁶⁰*Department of Physics, Indiana University, Bloomington, Indiana, USA*
- ⁶¹*Institut für Astro-und Teilchenphysik, Leopold-Franzens-Universität, Innsbruck, Austria*
- ⁶²*University of Iowa, Iowa City, Iowa, USA*
- ⁶³*Department of Physics and Astronomy, Iowa State University, Ames, Iowa, USA*
- ⁶⁴*Joint Institute for Nuclear Research, JINR Dubna, Dubna, Russia*
- ⁶⁵*KEK, High Energy Accelerator Research Organization, Tsukuba, Japan*
- ⁶⁶*Graduate School of Science, Kobe University, Kobe, Japan*
- ⁶⁷*Faculty of Science, Kyoto University, Kyoto, Japan*
- ⁶⁸*Kyoto University of Education, Kyoto, Japan*
- ⁶⁹*Department of Physics, Kyushu University, Fukuoka, Japan*
- ⁷⁰*Instituto de Física La Plata, Universidad Nacional de La Plata and CONICET, La Plata, Argentina*
- ⁷¹*Physics Department, Lancaster University, Lancaster, United Kingdom*
- ^{72a}*INFN Sezione di Lecce, Italy*
- ^{72b}*Dipartimento di Matematica e Fisica, Università del Salento, Lecce, Italy*
- ⁷³*Oliver Lodge Laboratory, University of Liverpool, Liverpool, United Kingdom*
- ⁷⁴*Department of Physics, Jožef Stefan Institute and University of Ljubljana, Ljubljana, Slovenia*
- ⁷⁵*School of Physics and Astronomy, Queen Mary University of London, London, United Kingdom*
- ⁷⁶*Department of Physics, Royal Holloway University of London, Surrey, United Kingdom*
- ⁷⁷*Department of Physics and Astronomy, University College London, London, United Kingdom*
- ⁷⁸*Louisiana Tech University, Ruston LA, USA*
- ⁷⁹*Laboratoire de Physique Nucléaire et de Hautes Energies, UPMC and Université Paris-Diderot and CNRS/IN2P3, Paris, France*
- ⁸⁰*Fysiska institutionen, Lunds universitet, Lund, Sweden*

- ⁸¹*Departamento de Fisica Teorica C-15, Universidad Autonoma de Madrid, Madrid, Spain*
- ⁸²*Institut für Physik, Universität Mainz, Mainz, Germany*
- ⁸³*School of Physics and Astronomy, University of Manchester, Manchester, United Kingdom*
- ⁸⁴*CPPM, Aix-Marseille Université and CNRS/IN2P3, Marseille, France*
- ⁸⁵*Department of Physics, University of Massachusetts, Amherst, Massachusetts, USA*
- ⁸⁶*Department of Physics, McGill University, Montreal, QC, Canada*
- ⁸⁷*School of Physics, University of Melbourne, Victoria, Australia*
- ⁸⁸*Department of Physics, The University of Michigan, Ann Arbor, Michigan, USA*
- ⁸⁹*Department of Physics and Astronomy, Michigan State University, East Lansing, Michigan, USA*
- ^{90a}*INFN Sezione di Milano, Italy*
- ^{90b}*Dipartimento di Fisica, Università di Milano, Milano, Italy*
- ⁹¹*B.I. Stepanov Institute of Physics, National Academy of Sciences of Belarus, Minsk, Republic of Belarus*
- ⁹²*National Scientific and Educational Centre for Particle and High Energy Physics, Minsk, Republic of Belarus*
- ⁹³*Department of Physics, Massachusetts Institute of Technology, Cambridge, Massachusetts, USA*
- ⁹⁴*Group of Particle Physics, University of Montreal, Montreal, QC, Canada*
- ⁹⁵*P.N. Lebedev Institute of Physics, Academy of Sciences, Moscow, Russia*
- ⁹⁶*Institute for Theoretical and Experimental Physics (ITEP), Moscow, Russia*
- ⁹⁷*Moscow Engineering and Physics Institute (MEPhI), Moscow, Russia*
- ⁹⁸*D.V.Skobel'syn Institute of Nuclear Physics, M.V.Lomonosov Moscow State University, Moscow, Russia*
- ⁹⁹*Fakultät für Physik, Ludwig-Maximilians-Universität München, München, Germany*
- ¹⁰⁰*Max-Planck-Institut für Physik (Werner-Heisenberg-Institut), München, Germany*
- ¹⁰¹*Nagasaki Institute of Applied Science, Nagasaki, Japan*
- ¹⁰²*Graduate School of Science and Kobayashi-Maskawa Institute, Nagoya University, Nagoya, Japan*
- ^{103a}*INFN Sezione di Napoli, Italy*
- ^{103b}*Dipartimento di Fisica, Università di Napoli, Napoli, Italy*
- ¹⁰⁴*Department of Physics and Astronomy, University of New Mexico, Albuquerque, New Mexico, USA*
- ¹⁰⁵*Institute for Mathematics, Astrophysics and Particle Physics, Radboud University Nijmegen/Nikhef, Nijmegen, The Netherlands*
- ¹⁰⁶*Nikhef National Institute for Subatomic Physics and University of Amsterdam, Amsterdam, The Netherlands*
- ¹⁰⁷*Department of Physics, Northern Illinois University, DeKalb, Illinois, USA*
- ¹⁰⁸*Budker Institute of Nuclear Physics, SB RAS, Novosibirsk, Russia*
- ¹⁰⁹*Department of Physics, New York University, New York, New York, USA*
- ¹¹⁰*Ohio State University, Columbus, Ohio, USA*
- ¹¹¹*Faculty of Science, Okayama University, Okayama, Japan*
- ¹¹²*Homer L. Dodge Department of Physics and Astronomy, University of Oklahoma, Norman, Oklahoma, USA*
- ¹¹³*Department of Physics, Oklahoma State University, Stillwater, Oklahoma, USA*
- ¹¹⁴*Palacký University, RCPTM, Olomouc, Czech Republic*
- ¹¹⁵*Center for High Energy Physics, University of Oregon, Eugene, Oregon, USA*
- ¹¹⁶*LAL, Université Paris-Sud and CNRS/IN2P3, Orsay, France*
- ¹¹⁷*Graduate School of Science, Osaka University, Osaka, Japan*
- ¹¹⁸*Department of Physics, University of Oslo, Oslo, Norway*
- ¹¹⁹*Department of Physics, Oxford University, Oxford, United Kingdom*
- ^{120a}*INFN Sezione di Pavia, Italy*
- ^{120b}*Dipartimento di Fisica, Università di Pavia, Pavia, Italy*
- ¹²¹*Department of Physics, University of Pennsylvania, Philadelphia, Pennsylvania, USA*
- ¹²²*Petersburg Nuclear Physics Institute, Gatchina, Russia*
- ^{123a}*INFN Sezione di Pisa, Italy*
- ^{123b}*Dipartimento di Fisica E. Fermi, Università di Pisa, Pisa, Italy*
- ¹²⁴*Department of Physics and Astronomy, University of Pittsburgh, Pittsburgh, Pennsylvania, USA*
- ^{125a}*Laboratorio de Instrumentacao e Fisica Experimental de Particulas-LIP, Lisboa, Portugal*
- ^{125b}*Faculdade de Ciências, Universidade de Lisboa, Lisboa, Portugal*
- ^{125c}*Department of Physics, University of Coimbra, Coimbra, Portugal*
- ^{125d}*Centro de Física Nuclear da Universidade de Lisboa, Lisboa, Portugal*
- ^{125e}*Departamento de Fisica, Universidade do Minho, Braga, Portugal*
- ^{125f}*Departamento de Fisica Teorica y del Cosmos and CAFPE, Universidad de Granada, Granada, Spain*
- ^{125g}*Dep Fisica and CEFITEC of Faculdade de Ciencias e Tecnologia, Universidade Nova de Lisboa, Caparica, Portugal*

- ¹²⁶*Institute of Physics, Academy of Sciences of the Czech Republic, Praha, Czech Republic*
¹²⁷*Czech Technical University in Prague, Praha, Czech Republic*
¹²⁸*Faculty of Mathematics and Physics, Charles University in Prague, Praha, Czech Republic*
¹²⁹*State Research Center Institute for High Energy Physics, Protvino, Russia*
¹³⁰*Particle Physics Department, Rutherford Appleton Laboratory, Didcot, United Kingdom*
¹³¹*Physics Department, University of Regina, Regina, SK, Canada*
¹³²*Ritsumeikan University, Kusatsu, Shiga, Japan*
^{133a}*INFN Sezione di Roma, Italy*
^{133b}*Dipartimento di Fisica, Sapienza Università di Roma, Roma, Italy*
^{134a}*INFN Sezione di Roma Tor Vergata, Italy*
^{134b}*Dipartimento di Fisica, Università di Roma Tor Vergata, Roma, Italy*
^{135a}*INFN Sezione di Roma Tre, Italy*
^{135b}*Dipartimento di Matematica e Fisica, Università Roma Tre, Roma, Italy*
^{136a}*Faculté des Sciences Ain Chock, Réseau Universitaire de Physique des Hautes Energies-Université Hassan II, Casablanca, Morocco*
^{136b}*Centre National de l'Energie des Sciences Techniques Nucleaires, Rabat, Morocco*
^{136c}*Faculté des Sciences Semlalia, Université Cadi Ayyad, LPHEA-Marrakech, Morocco*
^{136d}*Faculté des Sciences, Université Mohamed Premier and LPTPM, Oujda, Morocco*
^{136e}*Faculté des sciences, Université Mohammed V-Agdal, Rabat, Morocco*
¹³⁷*DSM/IRFU (Institut de Recherches sur les Lois Fondamentales de l'Univers), CEA Saclay (Commissariat à l'Energie Atomique et aux Energies Alternatives), Gif-sur-Yvette, France*
¹³⁸*Santa Cruz Institute for Particle Physics, University of California Santa Cruz, Santa Cruz, California, USA*
¹³⁹*Department of Physics, University of Washington, Seattle, Washington, USA*
¹⁴⁰*Department of Physics and Astronomy, University of Sheffield, Sheffield, United Kingdom*
¹⁴¹*Department of Physics, Shinshu University, Nagano, Japan*
¹⁴²*Fachbereich Physik, Universität Siegen, Siegen, Germany*
¹⁴³*Department of Physics, Simon Fraser University, Burnaby, BC, Canada*
¹⁴⁴*SLAC National Accelerator Laboratory, Stanford, California, USA*
^{145a}*Faculty of Mathematics, Physics & Informatics, Comenius University, Bratislava, Slovak Republic*
^{145b}*Department of Subnuclear Physics, Institute of Experimental Physics of the Slovak Academy of Sciences, Kosice, Slovak Republic*
^{146a}*Department of Physics, University of Cape Town, Cape Town, South Africa*
^{146b}*Department of Physics, University of Johannesburg, Johannesburg, South Africa*
^{146c}*School of Physics, University of the Witwatersrand, Johannesburg, South Africa*
^{147a}*Department of Physics, Stockholm University, Sweden*
^{147b}*The Oskar Klein Centre, Stockholm, Sweden*
¹⁴⁸*Physics Department, Royal Institute of Technology, Stockholm, Sweden*
¹⁴⁹*Departments of Physics&Astronomy and Chemistry, Stony Brook University, Stony Brook, New York, USA*
¹⁵⁰*Department of Physics and Astronomy, University of Sussex, Brighton, United Kingdom*
¹⁵¹*School of Physics, University of Sydney, Sydney, Australia*
¹⁵²*Institute of Physics, Academia Sinica, Taipei, Taiwan*
¹⁵³*Department of Physics, Technion: Israel Institute of Technology, Haifa, Israel*
¹⁵⁴*Raymond and Beverly Sackler School of Physics and Astronomy, Tel Aviv University, Tel Aviv, Israel*
¹⁵⁵*Department of Physics, Aristotle University of Thessaloniki, Thessaloniki, Greece*
¹⁵⁶*International Center for Elementary Particle Physics and Department of Physics, The University of Tokyo, Tokyo, Japan*
¹⁵⁷*Graduate School of Science and Technology, Tokyo Metropolitan University, Tokyo, Japan*
¹⁵⁸*Department of Physics, Tokyo Institute of Technology, Tokyo, Japan*
¹⁵⁹*Department of Physics, University of Toronto, Toronto, Ontario, Canada*
^{160a}*TRIUMF, Vancouver, BC, Canada*
^{160b}*Department of Physics and Astronomy, York University, Toronto, ON, Canada*
¹⁶¹*Faculty of Pure and Applied Sciences, University of Tsukuba, Tsukuba, Japan*
¹⁶²*Department of Physics and Astronomy, Tufts University, Medford, Massachusetts, USA*
¹⁶³*Centro de Investigaciones, Universidad Antonio Narino, Bogota, Colombia*
¹⁶⁴*Department of Physics and Astronomy, University of California Irvine, Irvine, CA, USA*
^{165a}*INFN Gruppo Collegato di Udine, Sezione di Trieste, Udine, Italy*
^{165b}*ICTP, Trieste, Italy*
^{165c}*Dipartimento di Chimica, Fisica e Ambiente, Università di Udine, Udine, Italy*

- ¹⁶⁶*Department of Physics, University of Illinois, Urbana, Illinois, USA*
- ¹⁶⁷*Department of Physics and Astronomy, University of Uppsala, Uppsala, Sweden*
- ¹⁶⁸*Instituto de Física Corpuscular (IFIC) and Departamento de Física Atómica, Molecular y Nuclear and Departamento de Ingeniería Electrónica and Instituto de Microelectrónica de Barcelona (IMB-CNM), University of Valencia and CSIC, Valencia, Spain*
- ¹⁶⁹*Department of Physics, University of British Columbia, Vancouver, BC, Canada*
- ¹⁷⁰*Department of Physics and Astronomy, University of Victoria, Victoria, BC, Canada*
- ¹⁷¹*Department of Physics, University of Warwick, Coventry, United Kingdom*
- ¹⁷²*Waseda University, Tokyo, Japan*
- ¹⁷³*Department of Particle Physics, The Weizmann Institute of Science, Rehovot, Israel*
- ¹⁷⁴*Department of Physics, University of Wisconsin, Madison, Wisconsin, USA*
- ¹⁷⁵*Fakultät für Physik und Astronomie, Julius-Maximilians-Universität, Würzburg, Germany*
- ¹⁷⁶*Fachbereich C Physik, Bergische Universität Wuppertal, Wuppertal, Germany*
- ¹⁷⁷*Department of Physics, Yale University, New Haven, Connecticut, USA*
- ¹⁷⁸*Yerevan Physics Institute, Yerevan, Armenia*
- ¹⁷⁹*Centre de Calcul de l'Institut National de Physique Nucléaire et de Physique des Particules (IN2P3), Villeurbanne, France*

^aDeceased.

^bAlso at Department of Physics, King's College London, London, United Kingdom.

^cAlso at Institute of Physics, Azerbaijan Academy of Sciences, Baku, Azerbaijan.

^dAlso at Particle Physics Department, Rutherford Appleton Laboratory, Didcot, United Kingdom.

^eAlso at TRIUMF, Vancouver, BC, Canada.

^fAlso at Department of Physics, California State University, Fresno, California, USA.

^gAlso at Tomsk State University, Tomsk, Russia.

^hAlso at CPPM, Aix-Marseille Université and CNRS/IN2P3, Marseille, France.

ⁱAlso at Università di Napoli Parthenope, Napoli, Italy.

^jAlso at Institute of Particle Physics (IPP), Canada.

^kAlso at Department of Physics, St. Petersburg State Polytechnical University, St. Petersburg, Russia.

^lAlso at Chinese University of Hong Kong, China.

^mAlso at Department of Financial and Management Engineering, University of the Aegean, Chios, Greece.

ⁿAlso at Louisiana Tech University, Ruston, Louisiana, USA.

^oAlso at Institutio Catalana de Recerca i Estudis Avancats, ICREA, Barcelona, Spain.

^pAlso at Department of Physics, The University of Texas at Austin, Austin, Texas, USA.

^qAlso at Institute of Theoretical Physics, Iliia State University, Tbilisi, Georgia.

^rAlso at CERN, Geneva, Switzerland.

^sAlso at Ochadai Academic Production, Ochanomizu University, Tokyo, Japan.

^tAlso at Manhattan College, New York, New York, USA.

^uAlso at Novosibirsk State University, Novosibirsk, Russia.

^vAlso at Institute of Physics, Academia Sinica, Taipei, Taiwan.

^wAlso at LAL, Université Paris-Sud and CNRS/IN2P3, Orsay, France.

^xAlso at Academia Sinica Grid Computing, Institute of Physics, Academia Sinica, Taipei, Taiwan.

^yAlso at Laboratoire de Physique Nucléaire et de Hautes Energies, UPMC and Université Paris-Diderot and CNRS/IN2P3, Paris, France.

^zAlso at School of Physical Sciences, National Institute of Science Education and Research, Bhubaneswar, India.

^{aa}Also at Dipartimento di Fisica, Sapienza Università di Roma, Roma, Italy.

^{bb}Also at Moscow Institute of Physics and Technology State University, Dolgoprudny, Russia.

^{cc}Also at Section de Physique, Université de Genève, Geneva, Switzerland.

^{dd}Also at International School for Advanced Studies (SISSA), Trieste, Italy.

^{ee}Also at Department of Physics and Astronomy, University of South Carolina, Columbia, South Carolina, USA.

^{ff}Also at School of Physics and Engineering, Sun Yat-sen University, Guangzhou, China.

^{gg}Also at Faculty of Physics, M.V.Lomonosov Moscow State University, Moscow, Russia.

^{hh}Also at Moscow Engineering and Physics Institute (MEPhI), Moscow, Russia.

ⁱⁱAlso at Institute for Particle and Nuclear Physics, Wigner Research Centre for Physics, Budapest, Hungary.

^{jj}Also at Department of Physics, Oxford University, Oxford, United Kingdom.

^{kk}Also at Department of Physics, Nanjing University, Jiangsu, China.

^{ll}Also at Institut für Experimentalphysik, Universität Hamburg, Hamburg, Germany.

^{mmm}Also at Department of Physics, The University of Michigan, Ann Arbor, Michigan, USA.

ⁿⁿAlso at Discipline of Physics, University of KwaZulu-Natal, Durban, South Africa.

^{oo}Also at University of Malaya, Department of Physics, Kuala Lumpur, Malaysia.